The Unique Power of Chandra Observations of Gravitationally Lensed Quasars

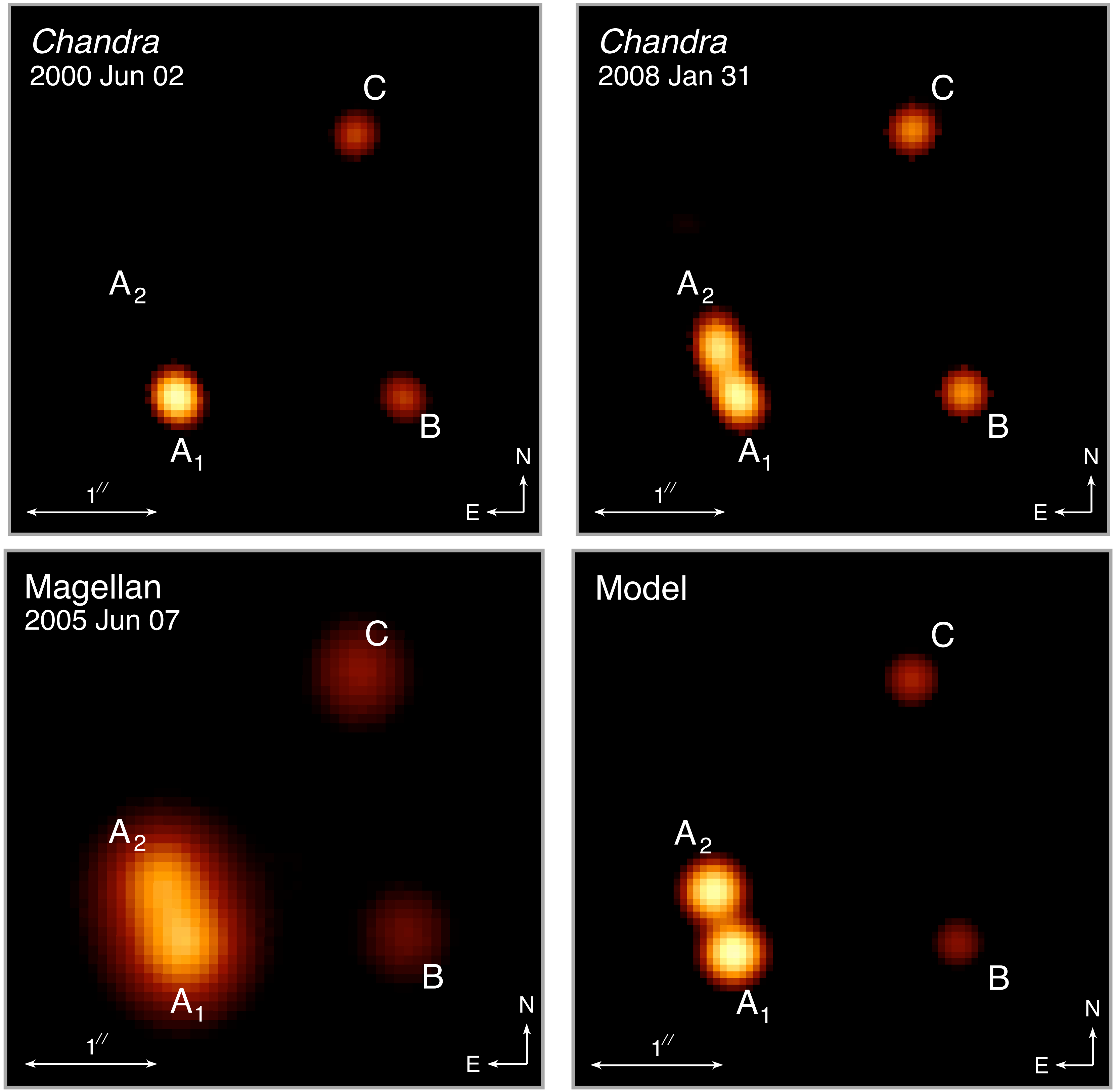

David Pooley
Trinity University
dpooley@trinity.edu

Paul Schechter (MIT)
Saul Rappaport (MIT)

PG 1115+080 X-rays, optical, and lens model

DP et al. 2008

Stronger X-ray anomalies are nearly universal, indicating microlensing is the cause.

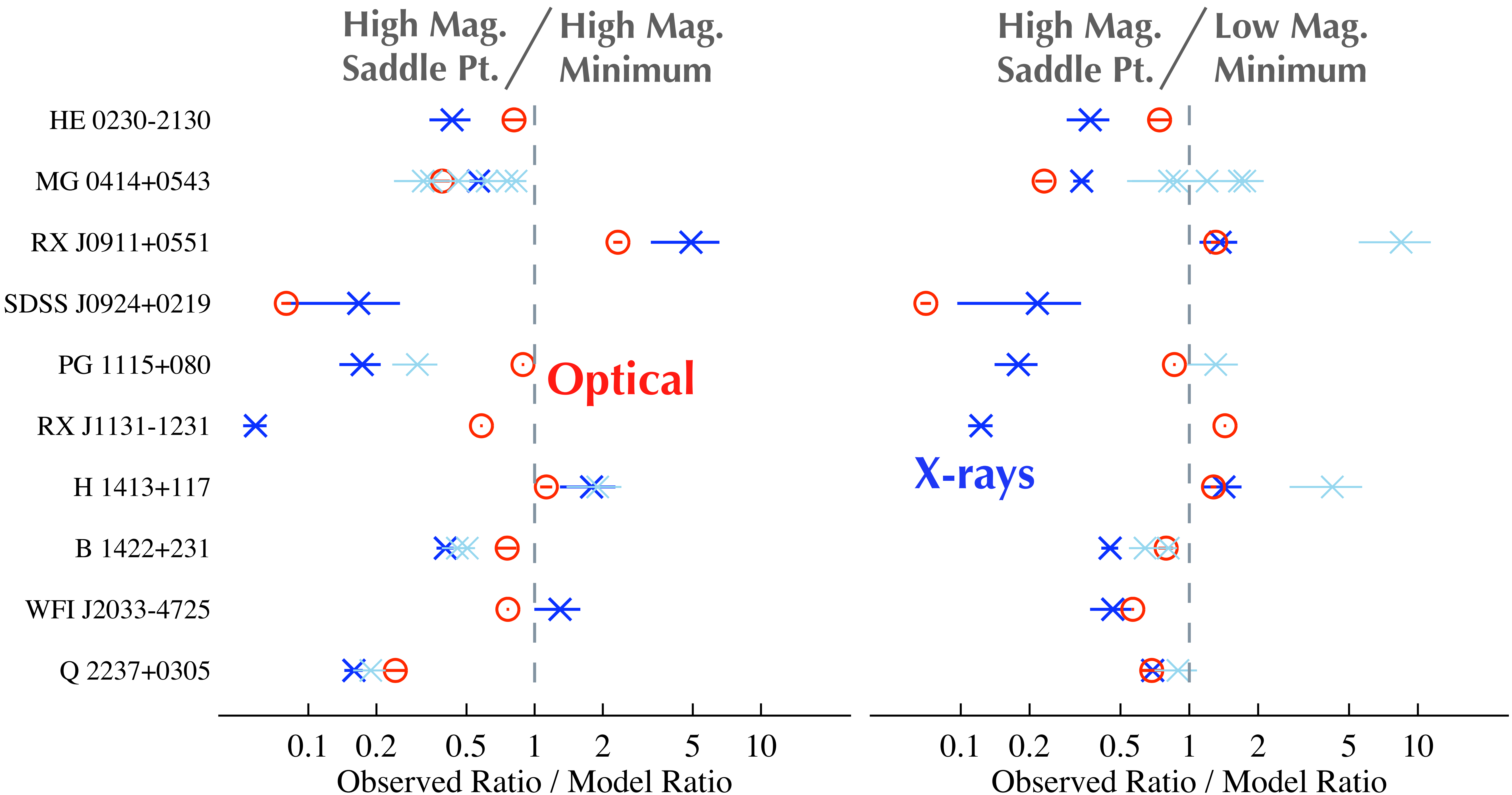

DP et al. 2007

Microlensing-induced variations diminish by ½ when source size ~ ⅓ lens size.

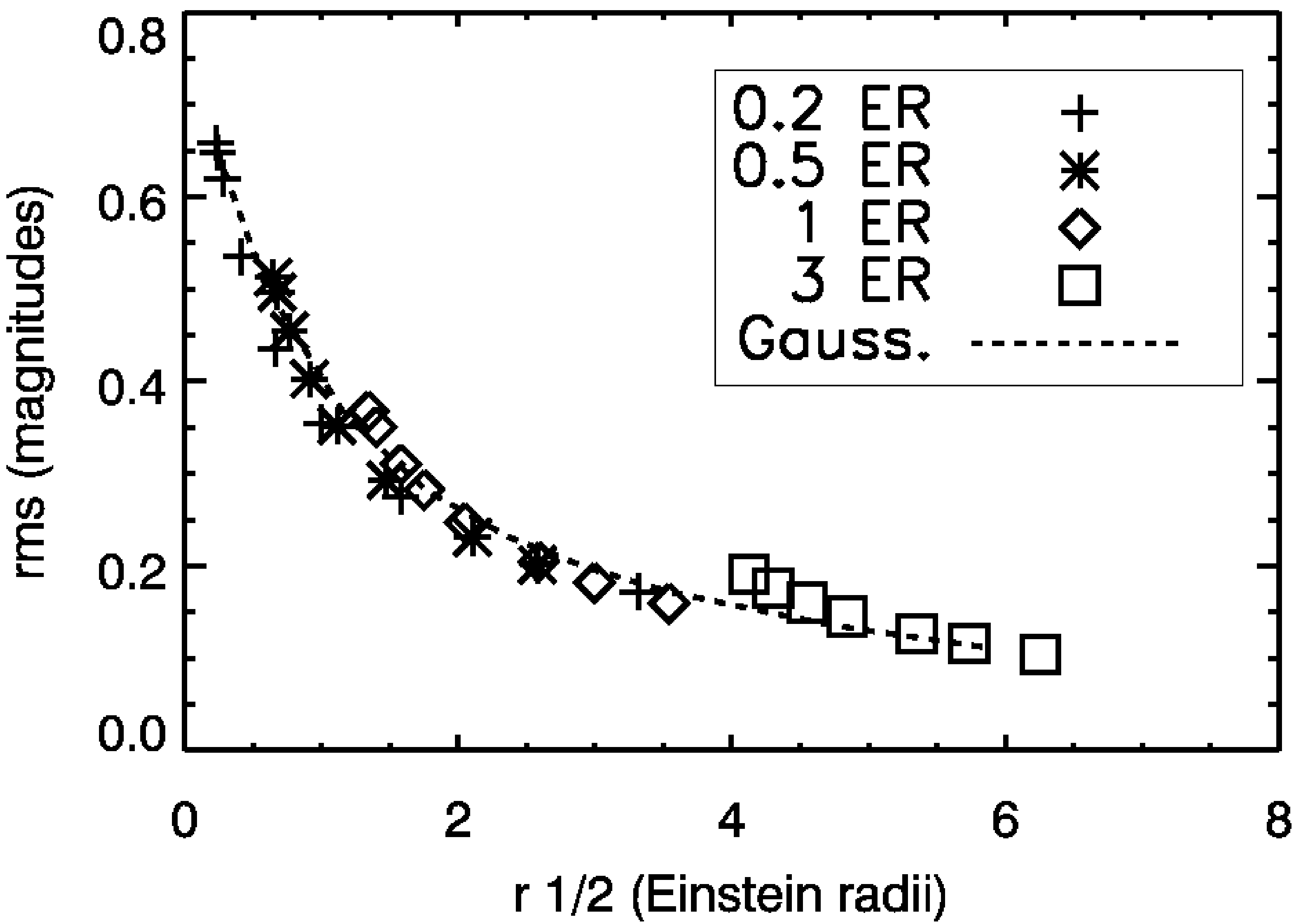

Mortonson, Schechter, & Wambsganss 2005

Optical RMS is roughly ½ the X-ray RMS. ➡ ***Optical region must be ⅓ size of the microlensing star.***

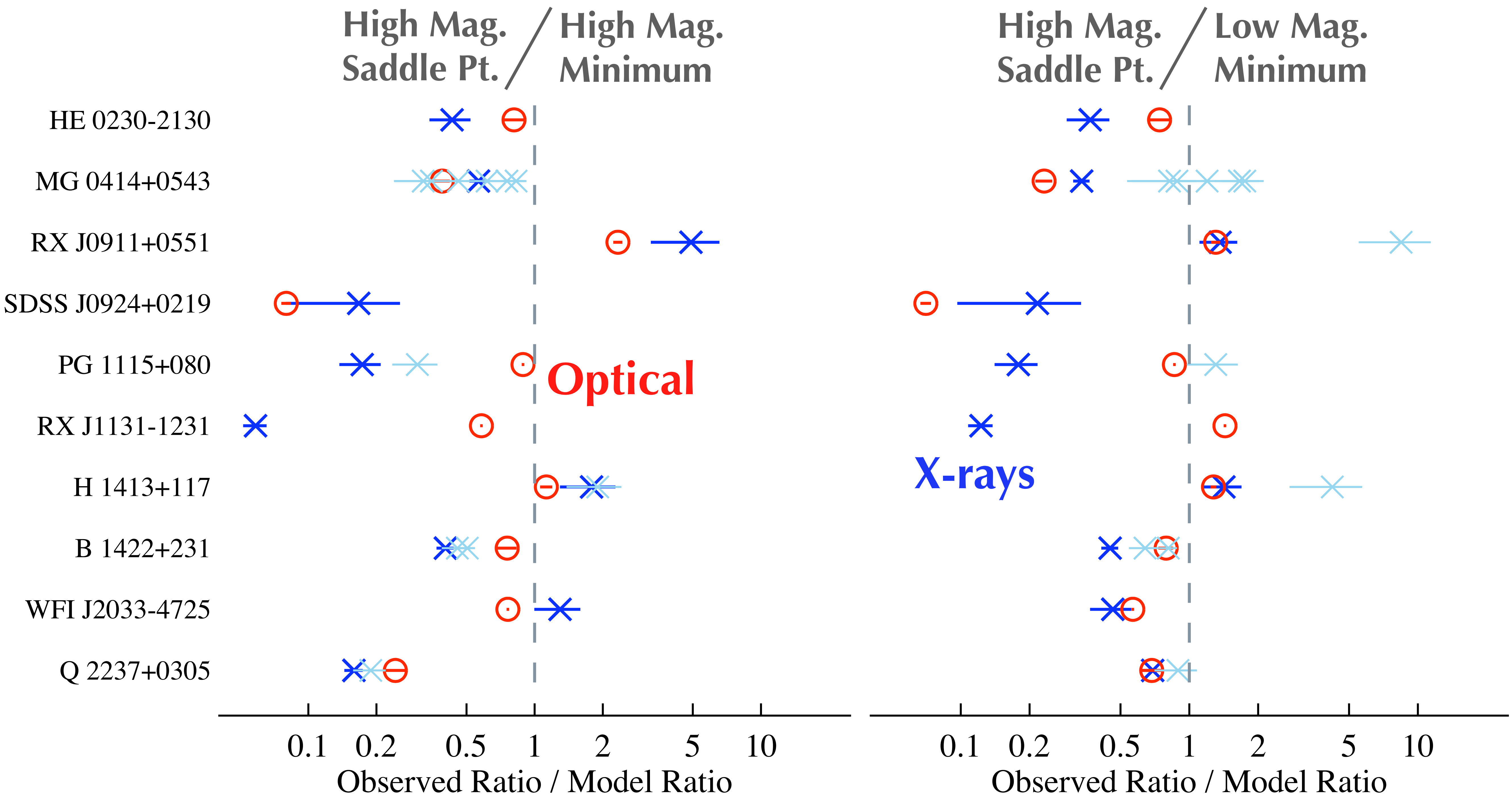

DP et al. 2007

This is not a single-star effect!

These two realizations of the stars in a ~60 microarcsecond field lensing a background quasar show all of the micro-images that go into forming one of the four macro images of the quasar.

The only difference is the position of the background quasar relative to the stars.

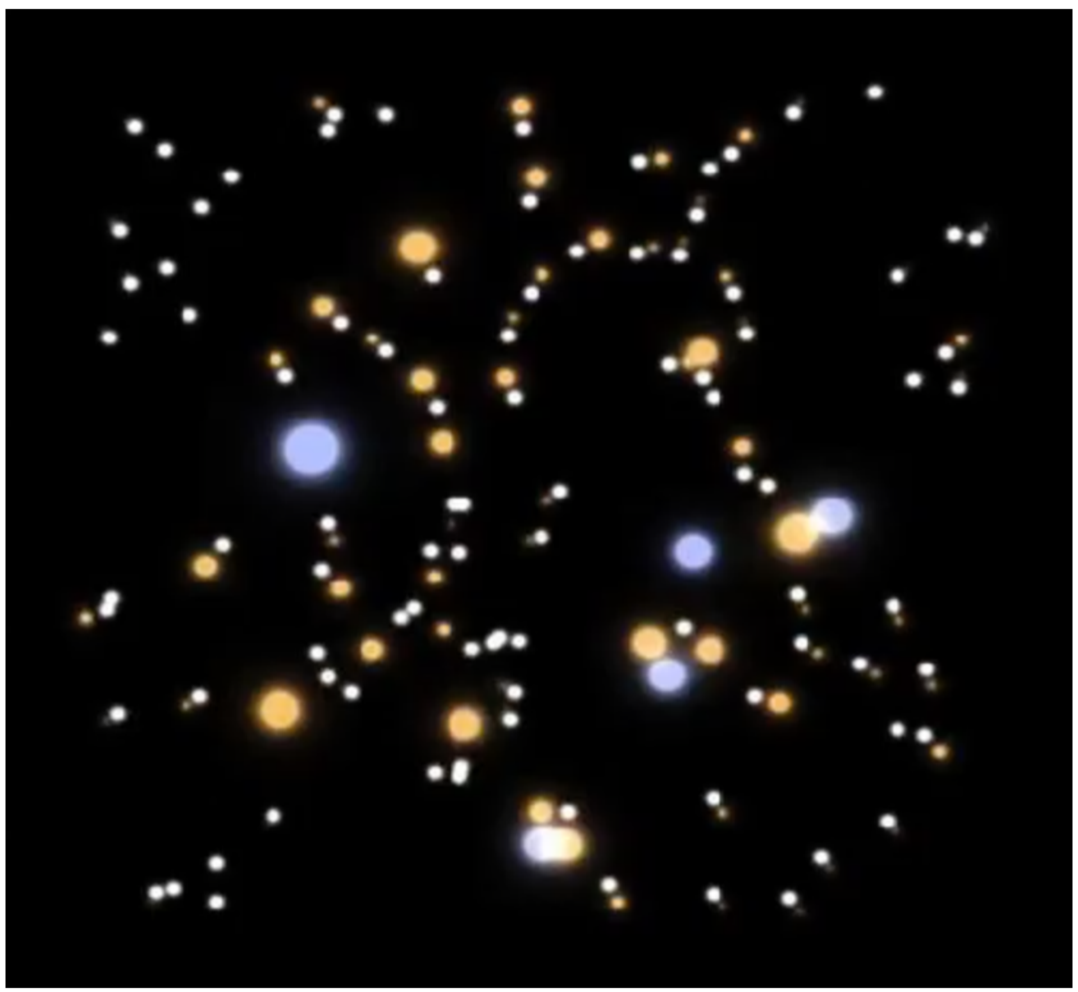

Magnification factor: ~5

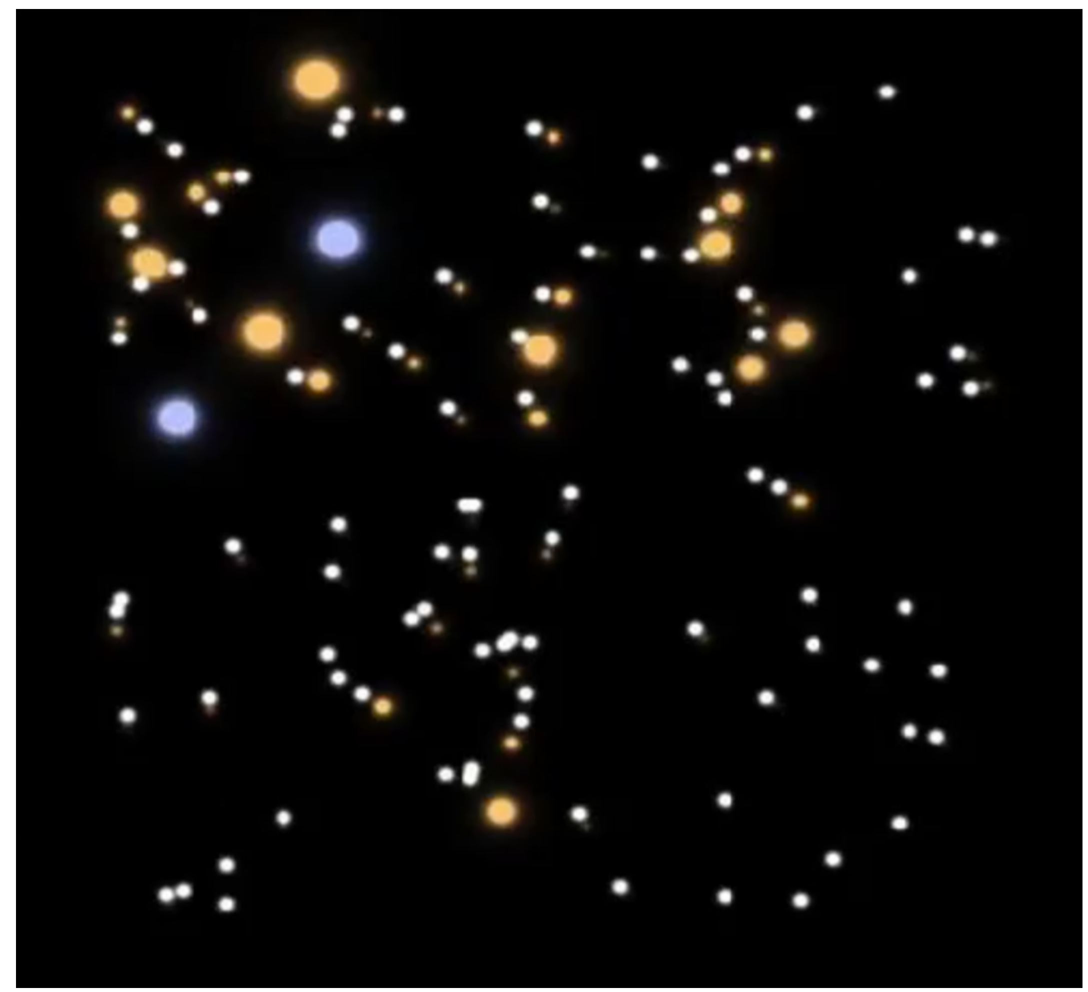

Magnification factor: ~2

see Paczynski 1986

This is not a single-star effect!

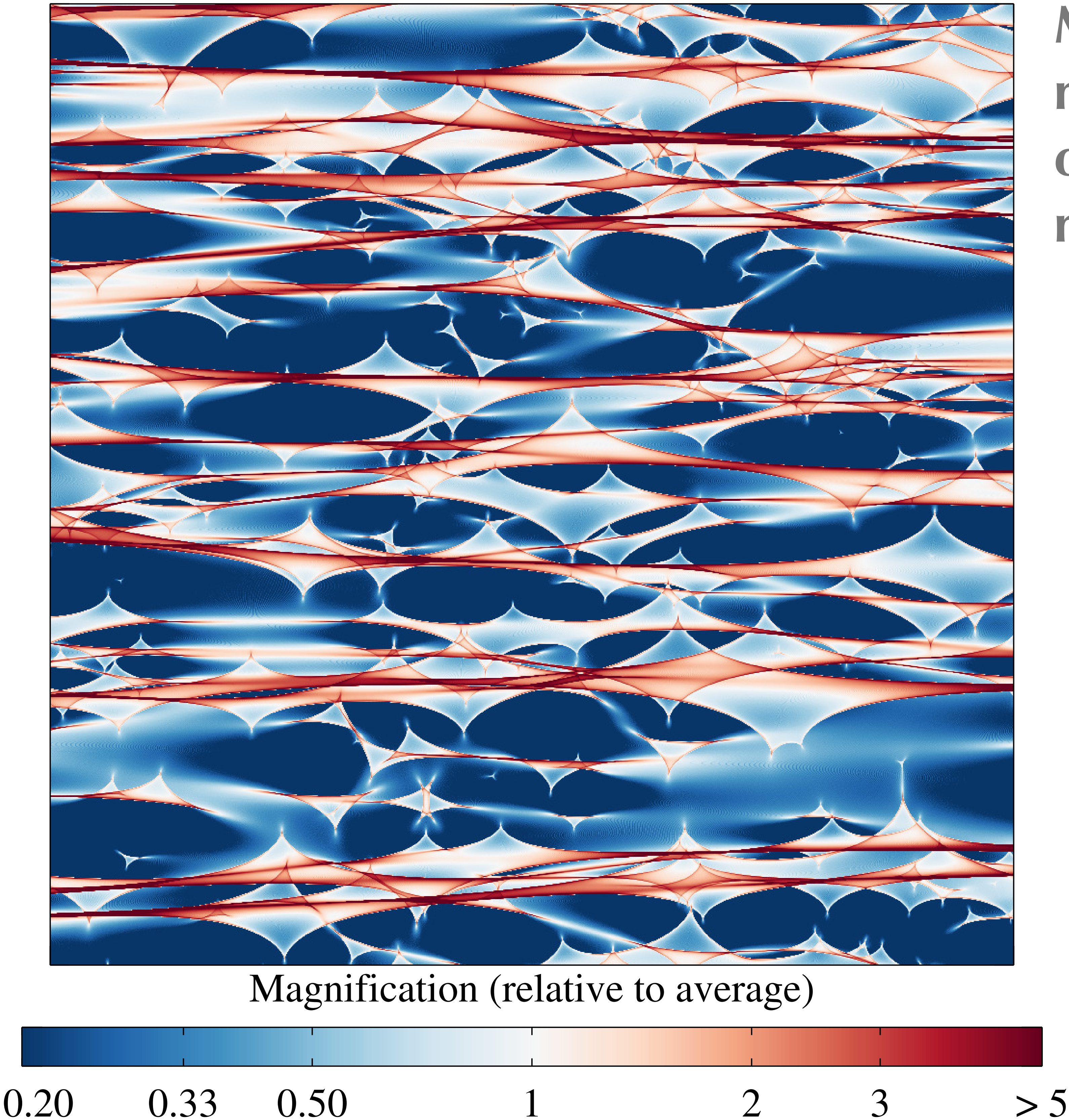

Microlensing magnification maps represent the effects of this "network" of microlensing stars.

Analysis of magnification maps gives probability of strong microlensing effects.

1% stars

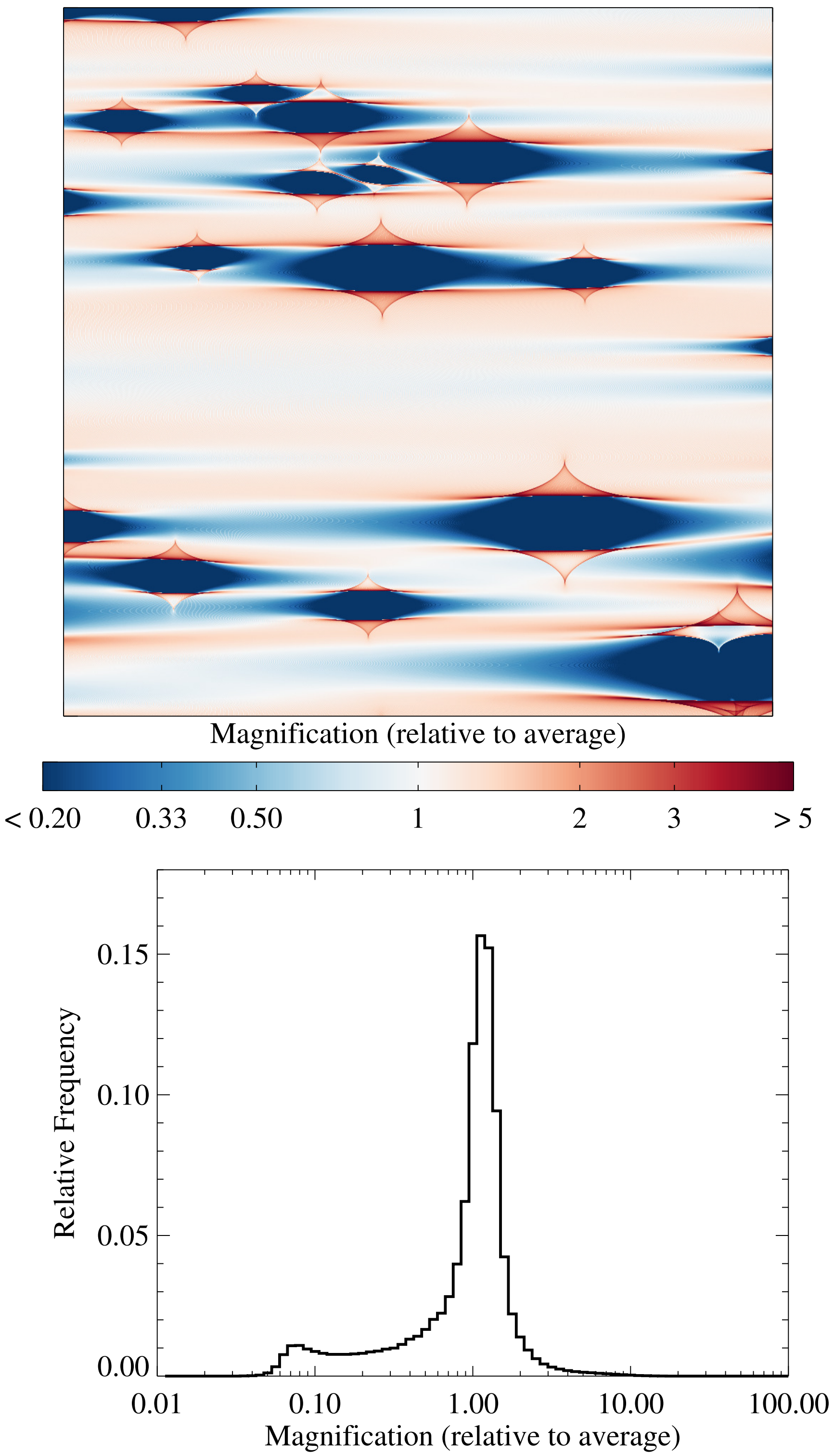

10% stars

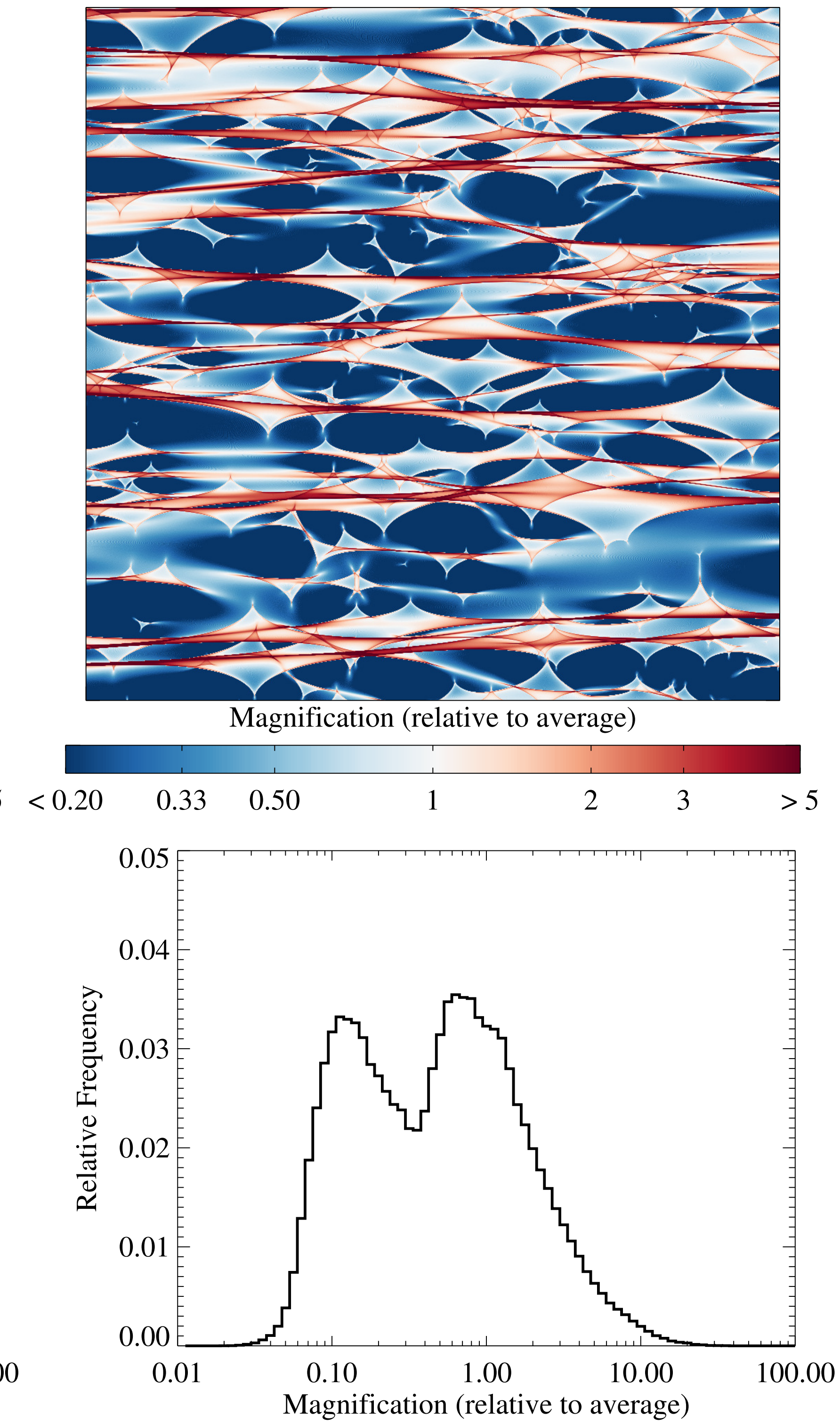

100% stars

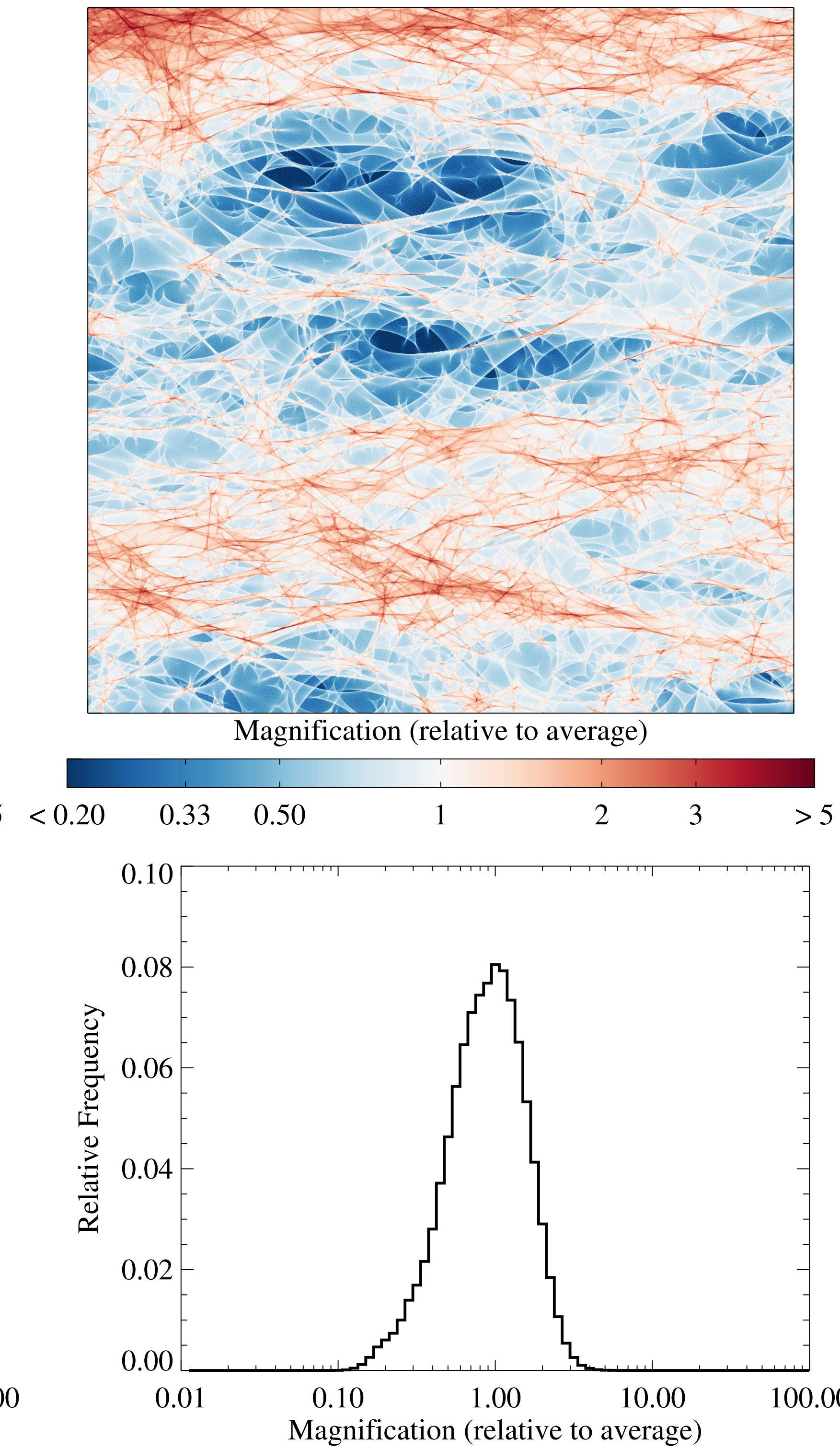

Ensemble of quads indicates 93% dark matter at $\langle R \rangle$ = 6.6 kpc

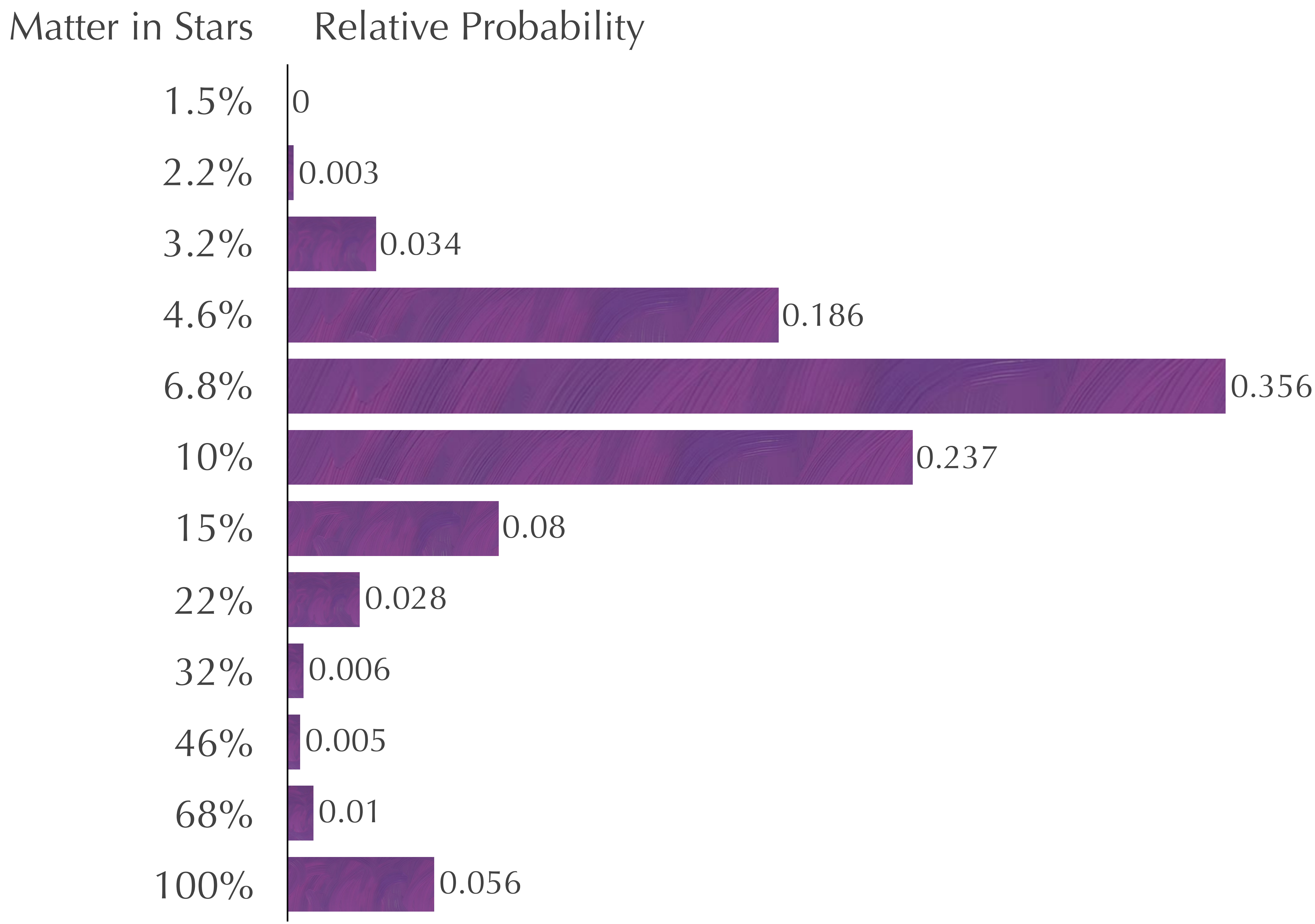

DP et al. 2012

Stellar Mass Density (M/L Ratio)

Knowing the overall mass density (from the lensing model) and the amount of mass in stars, one can estimate the stellar mass density.

We characterize this as a calibration factor that multiplies the stellar mass fundamental plane

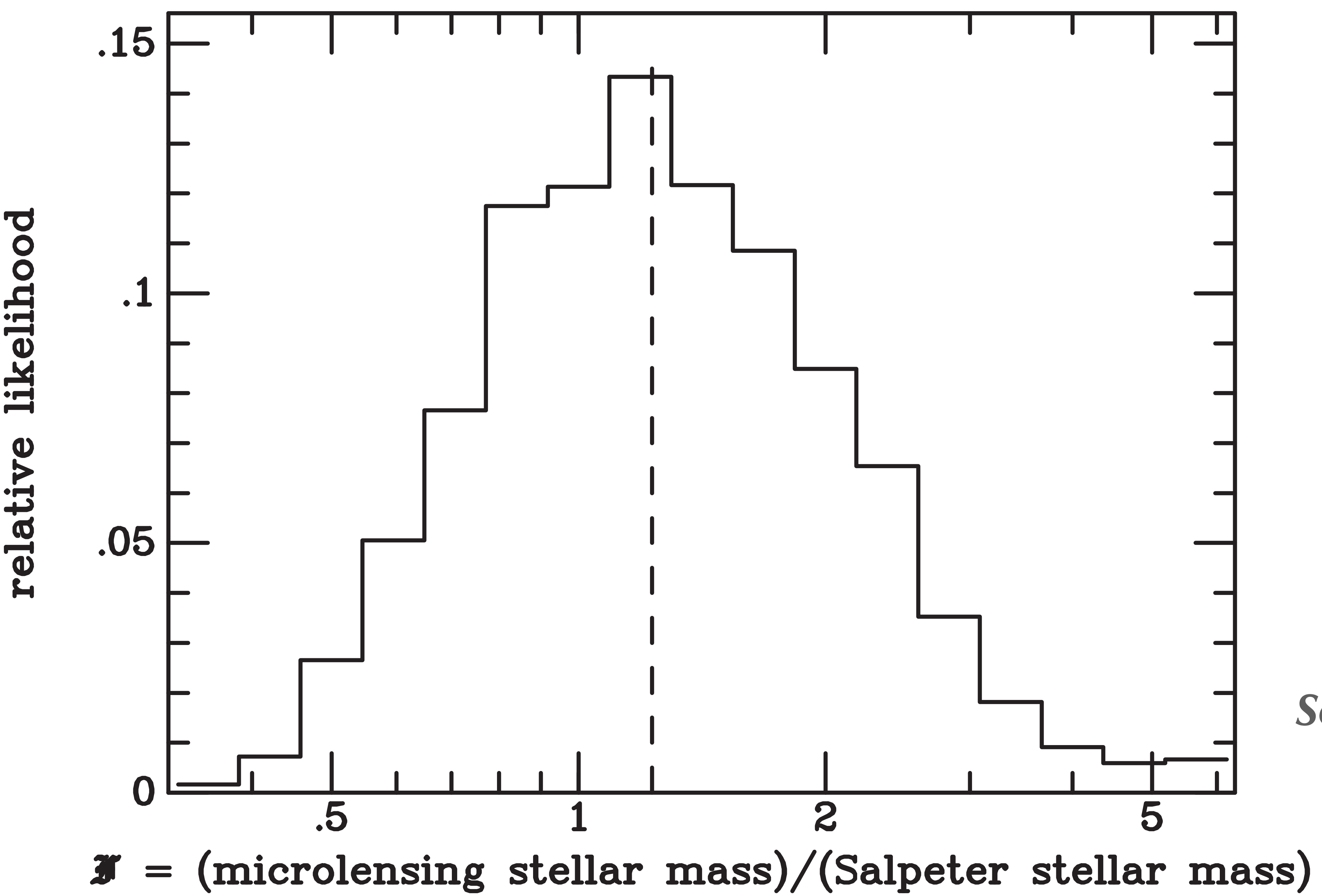

Schechter et al. 2014

Chandra Observations for the Next Decade

1. The discovery of new lensed quasars in large-area optical surveys will provide additional targets for *Chandra*, improving the ensemble results.
   - Size of optical region
   - DM fraction / stellar mass density

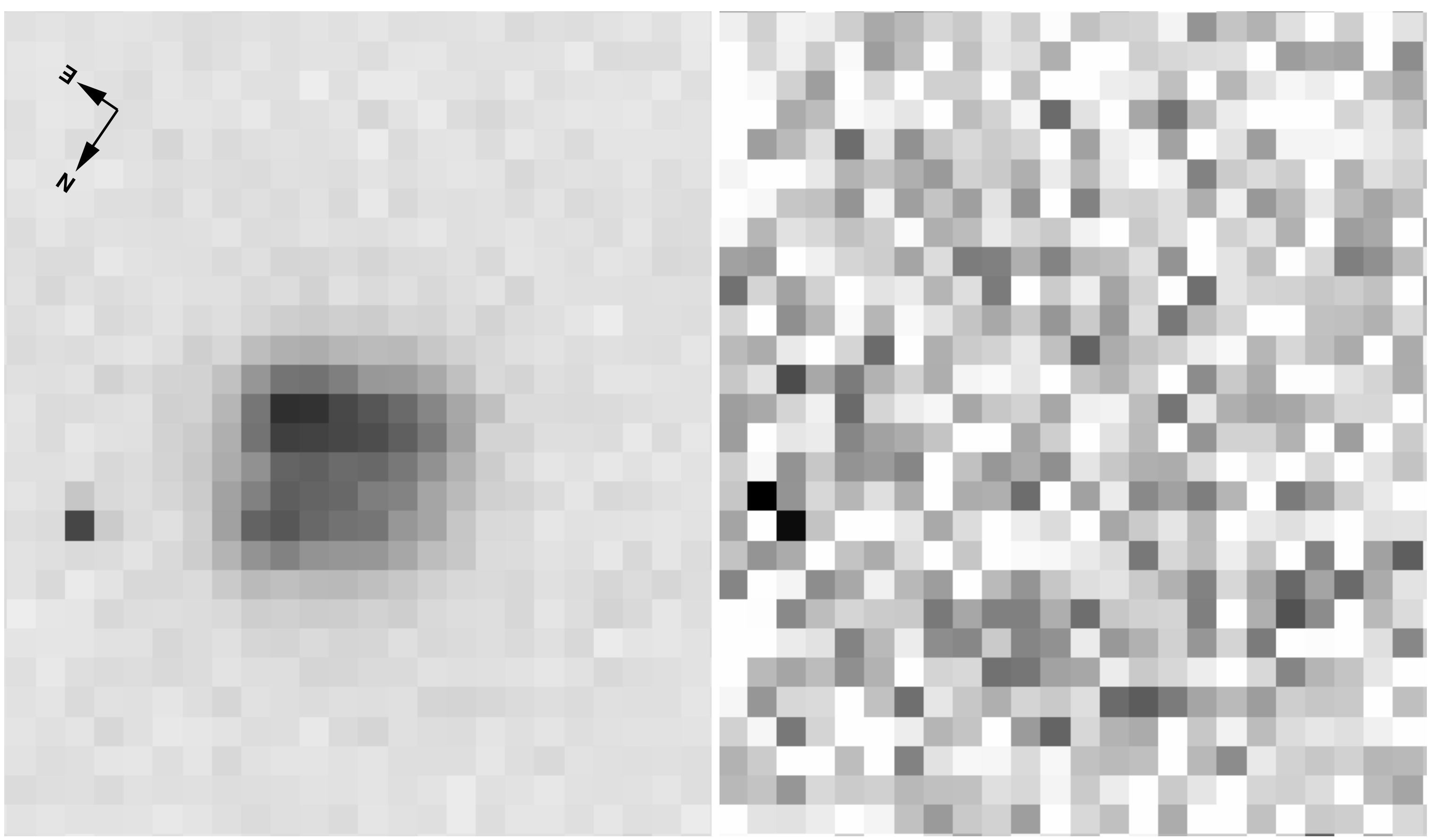

Fig. 2.— Left: A 60s i exposure of WISE 2344-3056 taken with IMACS in $0\farcs55$ seeing. Right: the same exposure, with four point sources subtracted, at 10 times higher contrast. The scale is $0\farcs200$ per pixel

VST-ATLAS discovery of WISE 2344-3056 as a quadruply lensed quasar.

Schechter et al. 2016

Chandra Observations for the Next Decade

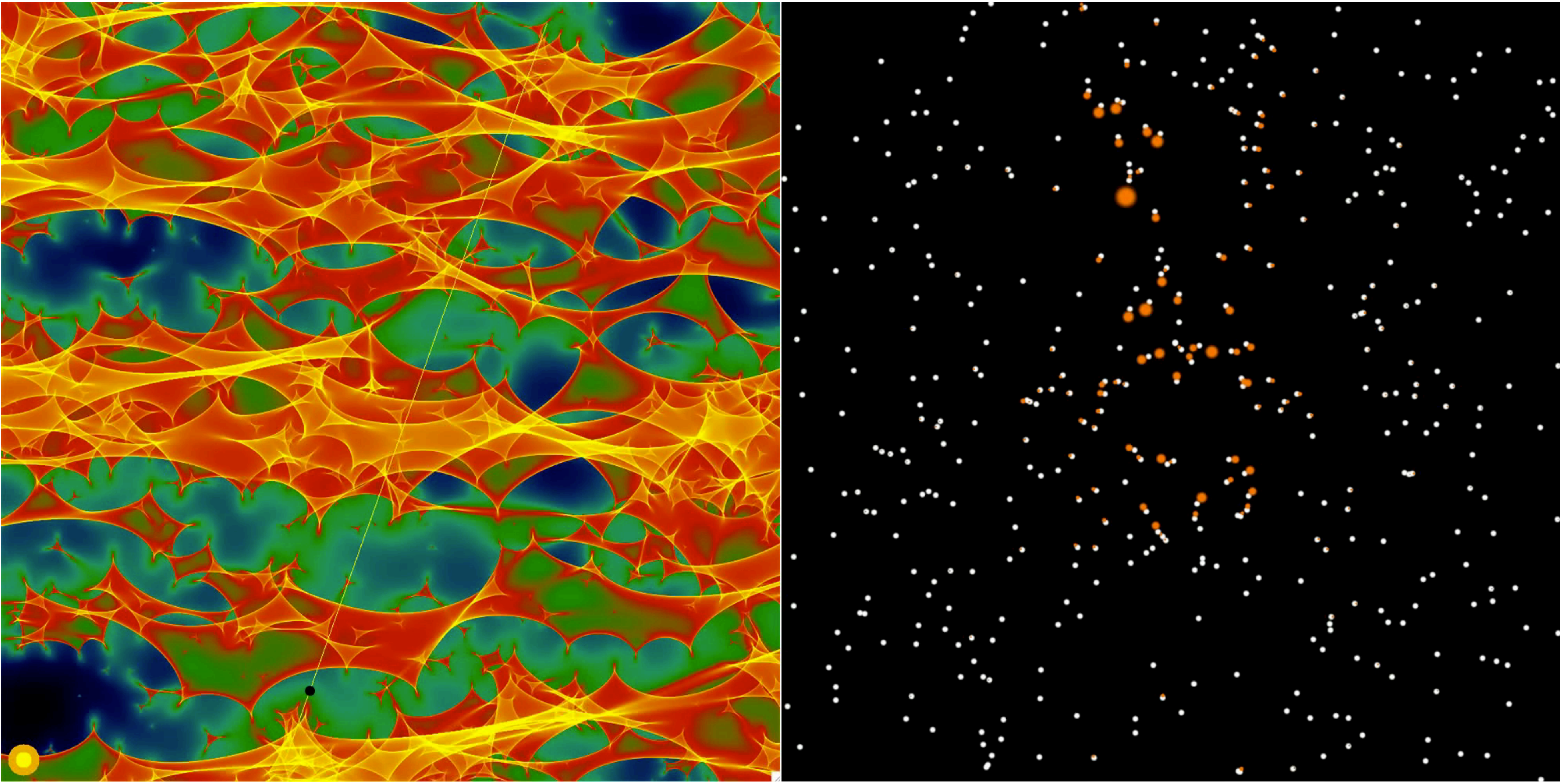

credit: Luke Weisenbach, MIT '18

Chandra Observations for the Next Decade

2. The dark matter fractions / stellar mass densities can be obtained for individual systems through repeated observations spaced by ~years. These would yield “independent” likelihood histograms, which could be combined in a way similar to the ensemble results.

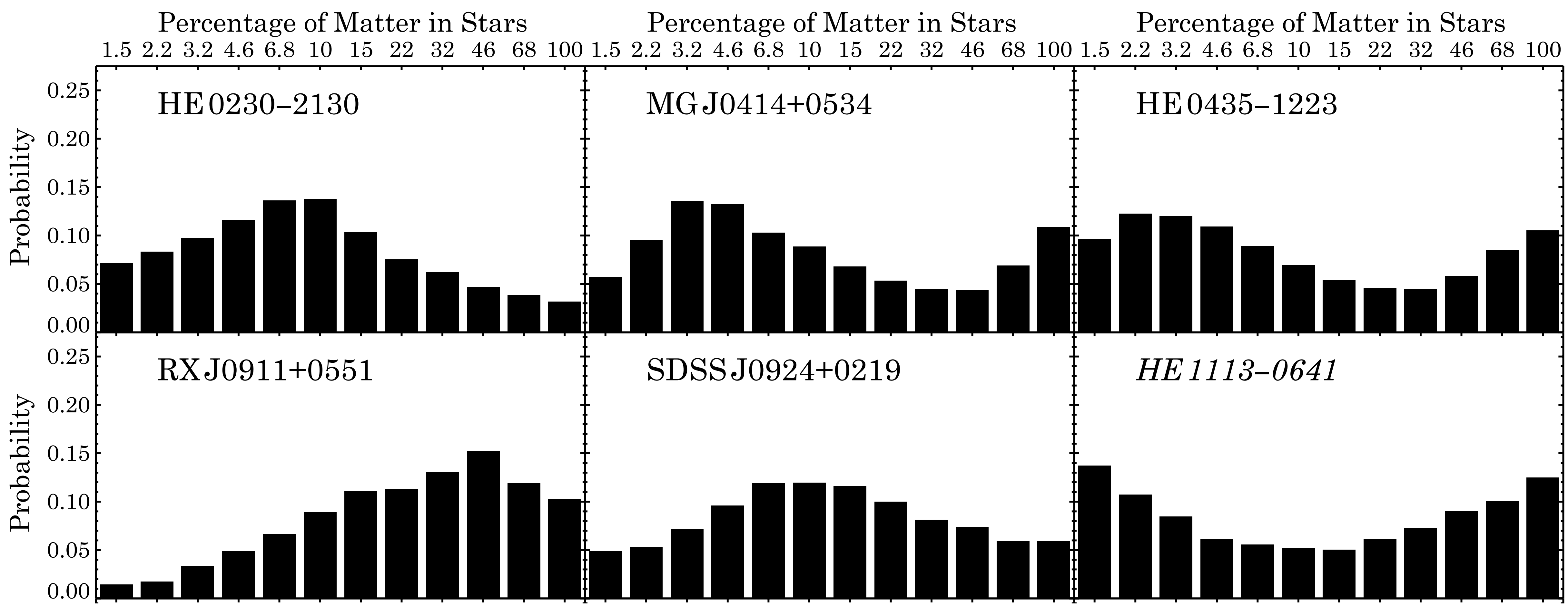

DP et al. 2012

Chandra Observations for the Next Decade

3. Dense sampling of caustic crossings can reveal the detailed structure of the X-ray emitting region.

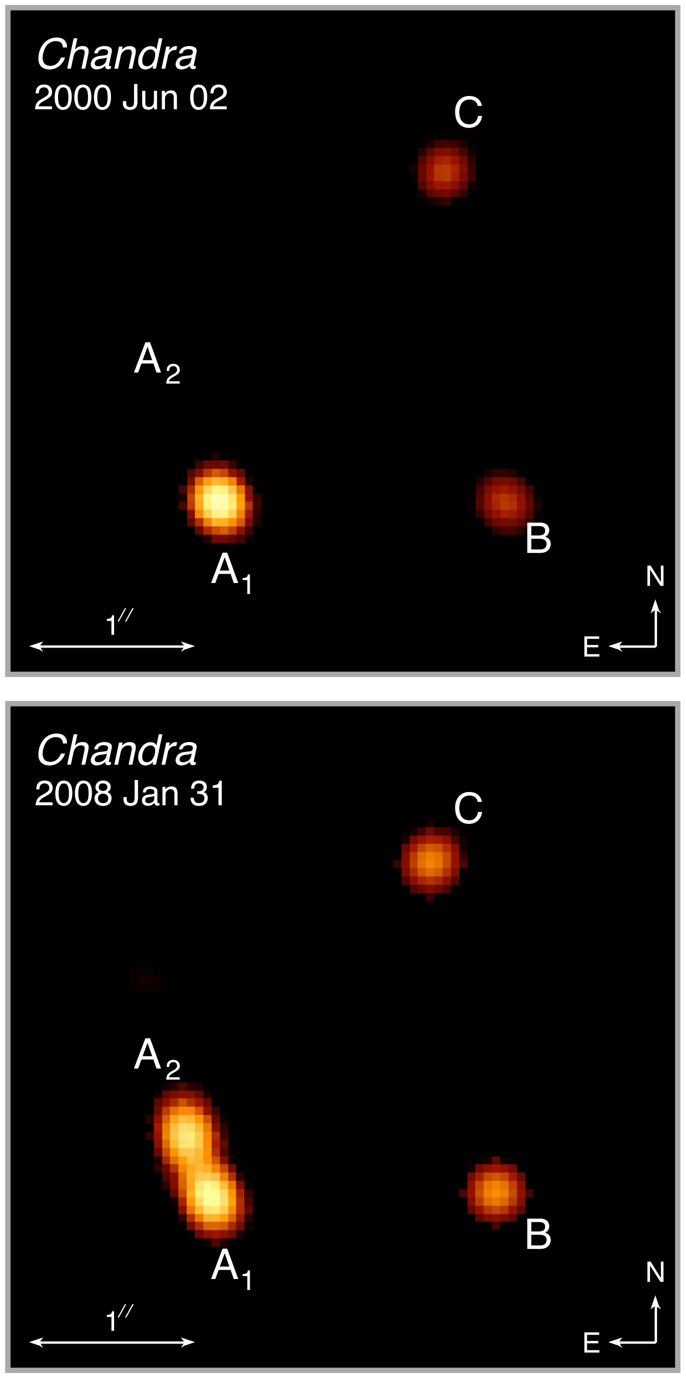

Likely caustic crossing in PG 1115+080

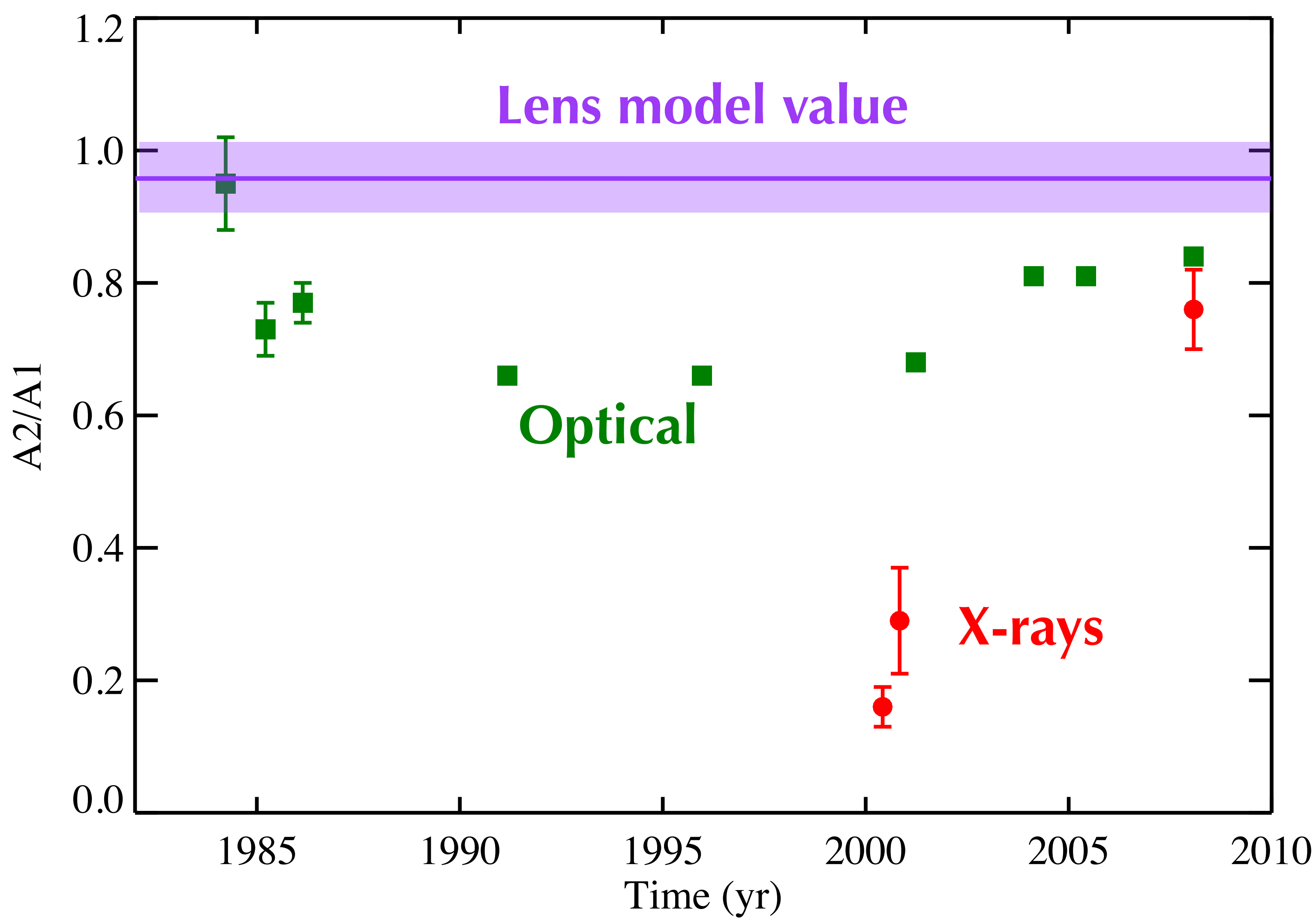

DP et al. 2008

Chandra Observations for the Next Decade

3. Dense sampling of caustic crossings can reveal the detailed structure of the X-ray emitting region.

Likely caustic crossing in HE 0230–2130

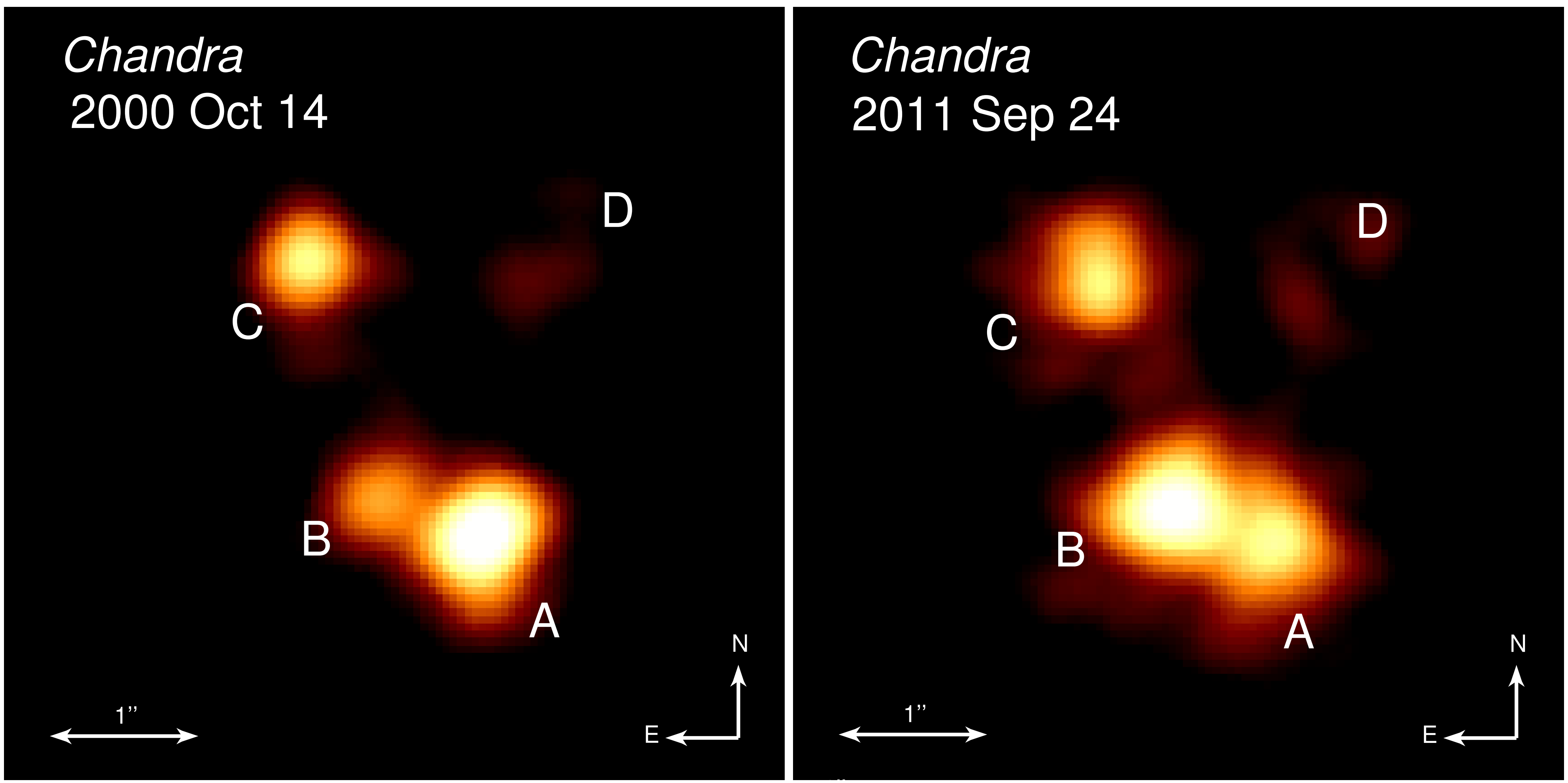

DP et al. in prep

Chandra Observations for the Next Decade

3. Dense sampling of caustic crossings can reveal the detailed structure of the X-ray emitting region.

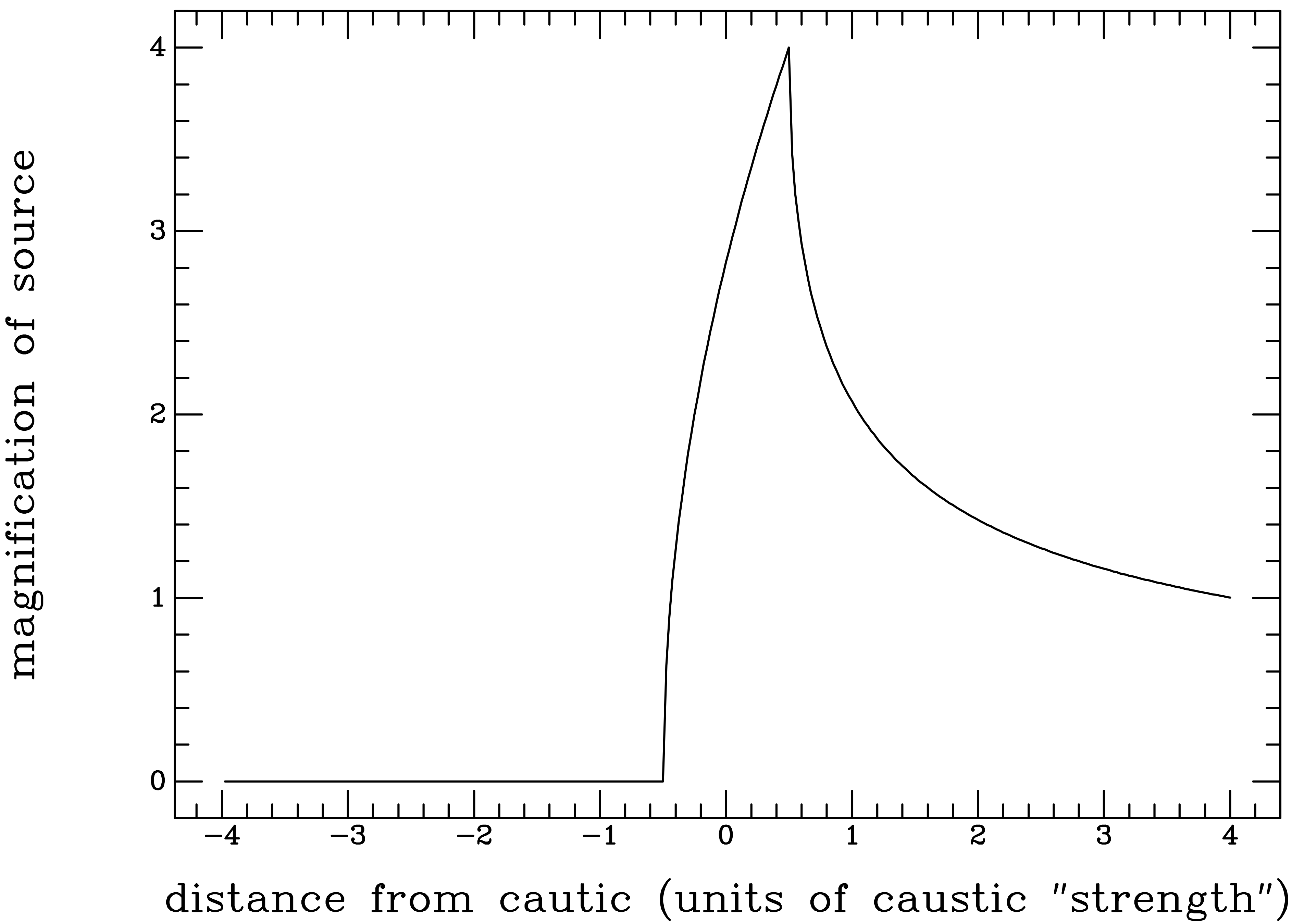

Chandra Observations for the Next Decade

3. Dense sampling of caustic crossings can reveal the detailed structure of the X-ray emitting region.

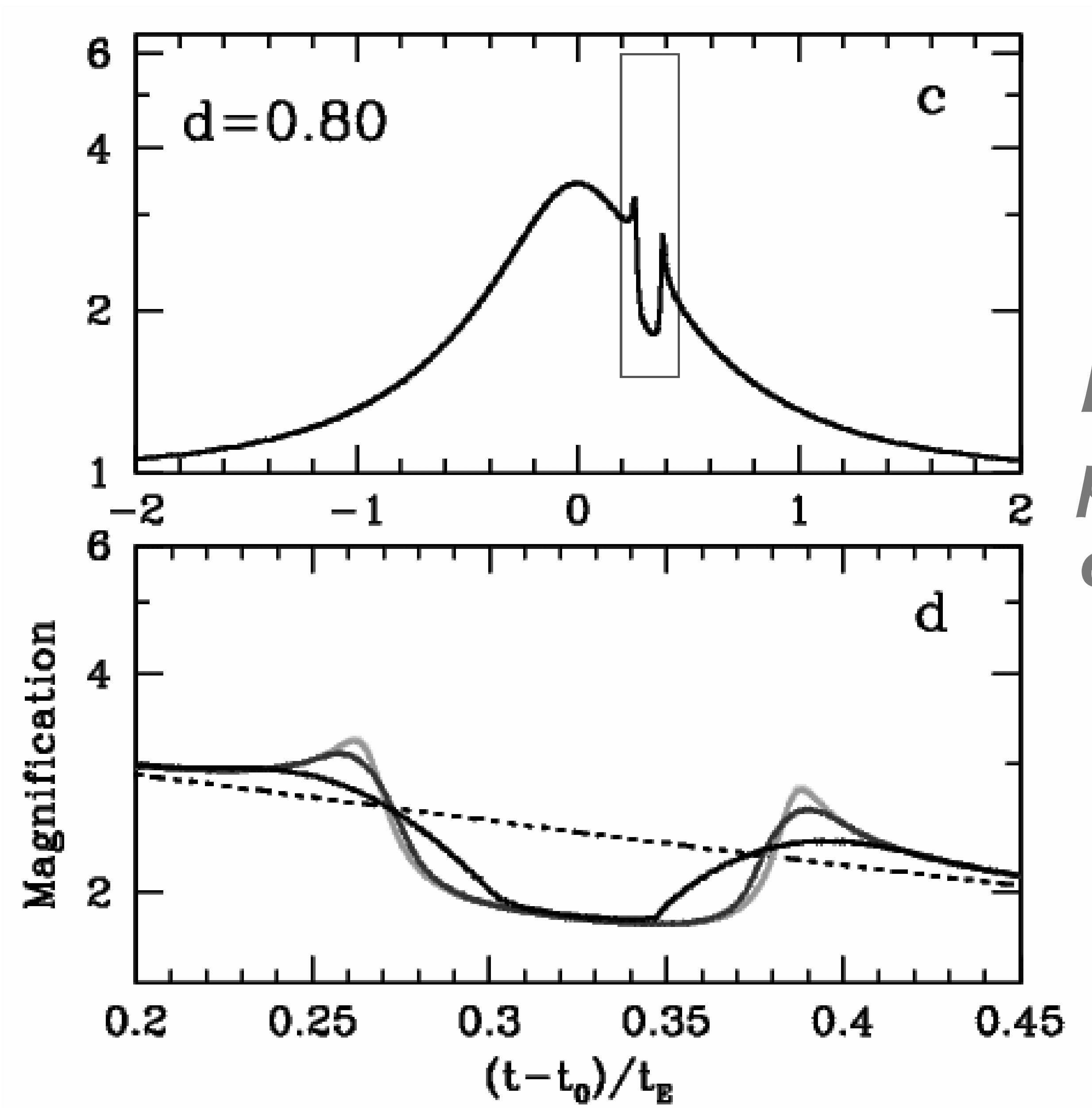

Gaudi 2010

Illustrative example from planetary microlensing shows effects of increasing source size.

Large anomalies were seen in the X-ray images.

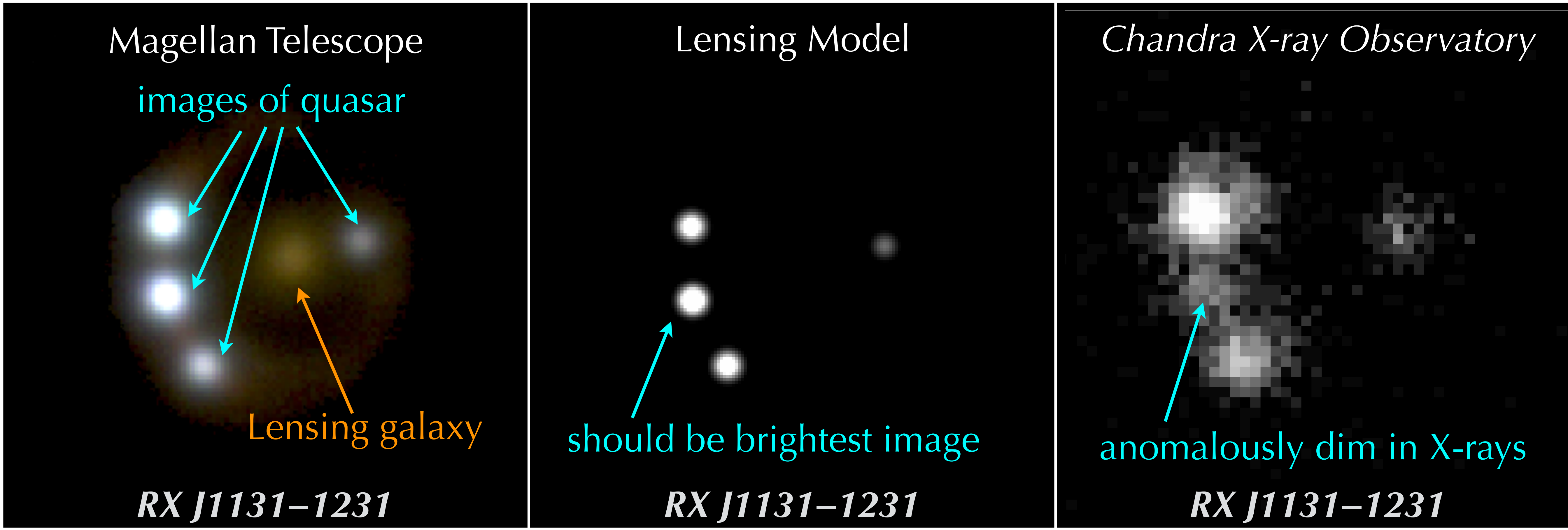

Blackburne, DP, & Rappaport 2006

These "flux ratio anomalies" were known in the optical for decades, but the explanation was unclear (*milli*lensing vs. *micro*lensing).

An optical emitting region that was large compared to the lens size was investigated by Schechter & Wambsganss (2004).

Improved X-ray data reduction gives more precise measurement.

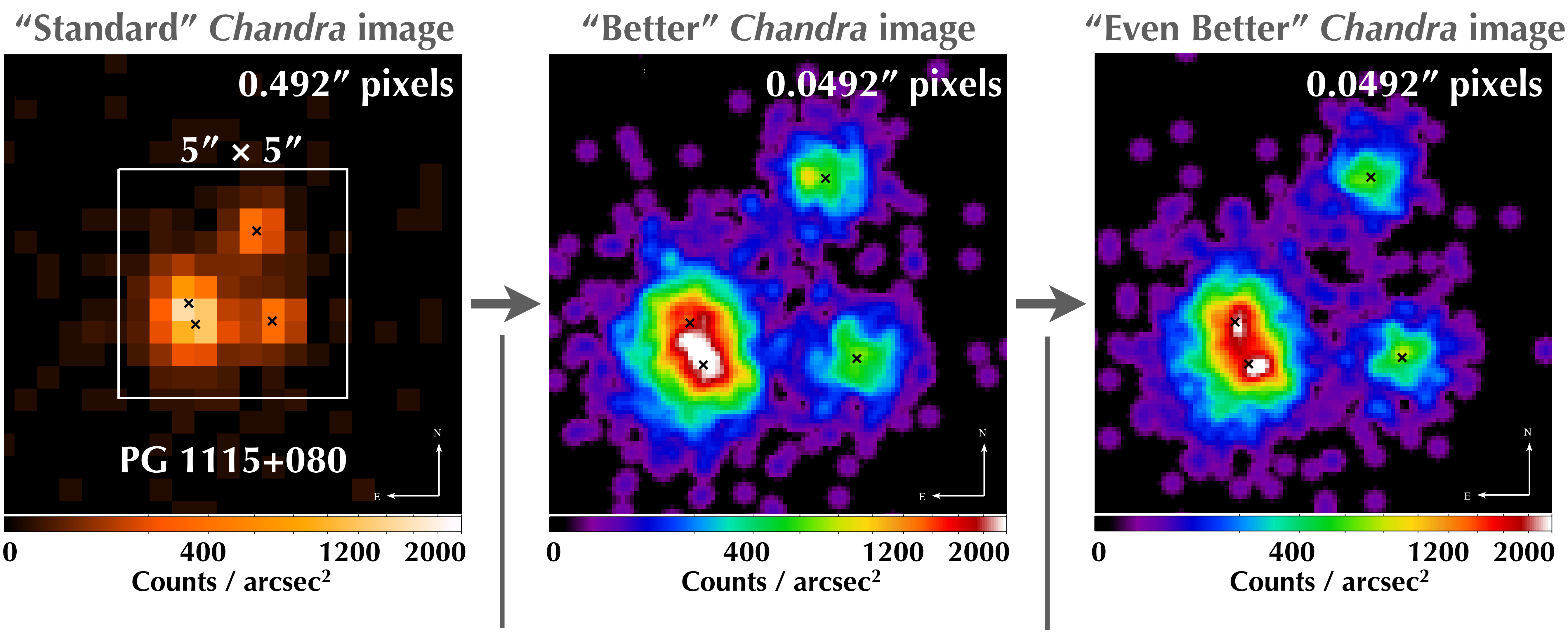

Use dithering of satellite

Use Sub-pixel Event Resolution

Position of an event is based on how charge cloud is split amongst neighboring pixels.

We calculate the optical $R_{1/2}$ for Shakura-Sunyaev disks and compare to the microlens Einstein radii:

Quasar	$L_{\mathrm{bol,opt}}$[a] (10^{45} erg s^{-1})	$L_{\mathrm{bol,X}}$[b] (10^{45} erg s^{-1})	$\log M_{\mathrm{BH}}$[c] ($M_\odot$)	$r_{1/2}$[d] (10^{15} cm)	$r_{1/2}$[d] (R_g)	stellar r_{Ein}[e] (10^{15} cm)	$\log r_{1/2}/r_{\mathrm{Ein}}$
HE 0230−2130	2.9	6.3	7.95 ± 0.24	0.93	70	43	-1.66 ± 0.16
MG J0414+0534	36	28	9.04 ± 0.17	3.8	23	31	-0.91 ± 0.11
RX J0911+0551	13	13	8.60 ± 0.18	1.9	32	35	-1.26 ± 0.12
SDSS J0924+0219	0.6	0.3	7.27 ± 0.56	0.42	152	48	-2.06 ± 0.37
PG 1115+080	11	6.6	8.53 ± 0.37	2.5	50	55	-1.35 ± 0.25
RX J1131−1231	0.80	1.3	7.39 ± 0.19	0.84	230	38	-1.65 ± 0.13
H 1413+117	56	6.5	9.24 ± 0.51	5.4	…	…	…
B 1422+231	250	135	9.89 ± 0.18	13	11	47	-0.55 ± 0.12
WFI J2033−4723	5.7	3.8	8.24 ± 0.12	1.6	62	36	-1.35 ± 0.08
Q 2237+0305	32	2.7	8.99 ± 0.76	5.5	38	150	-1.43 ± 0.51

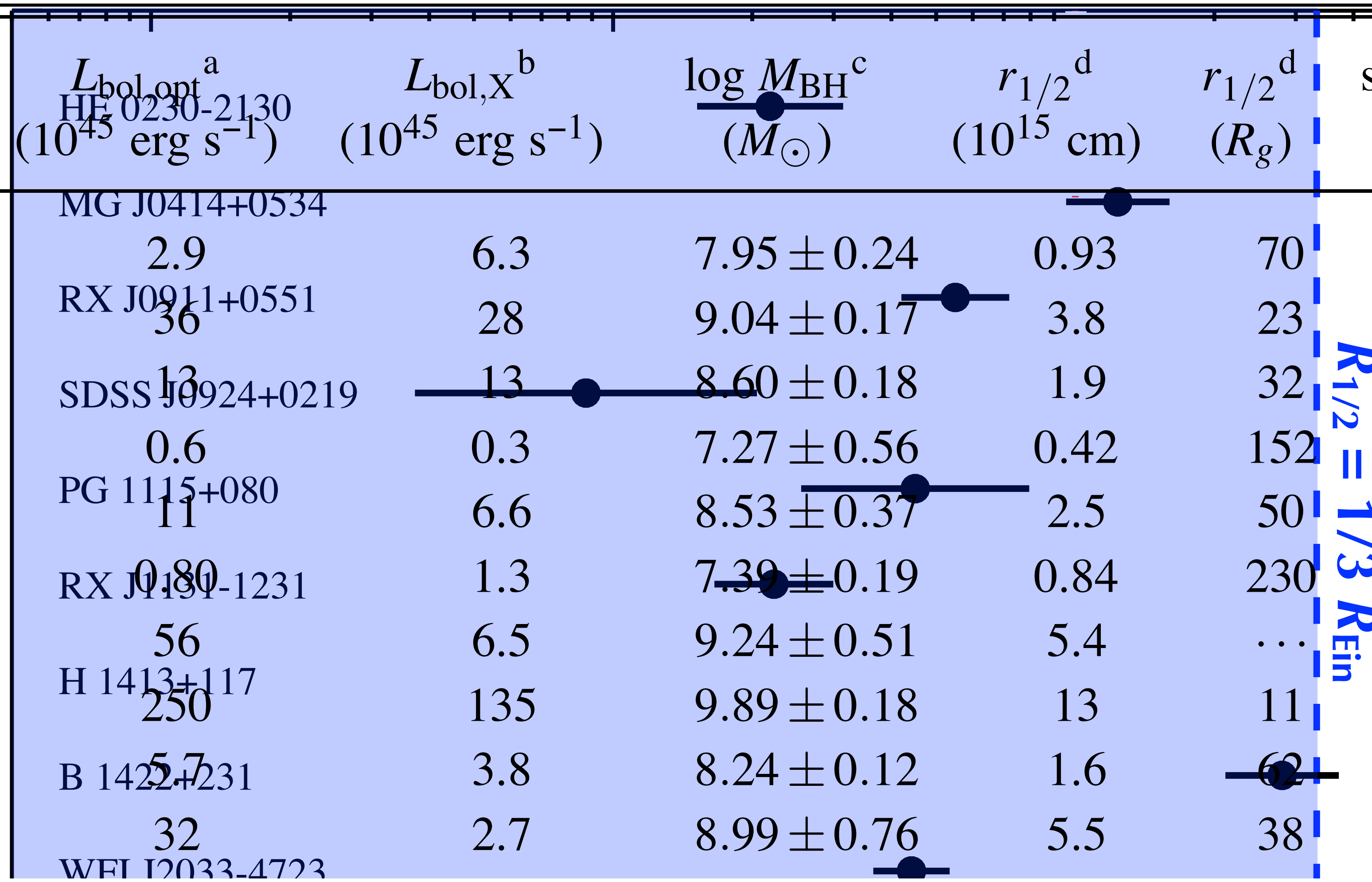

Probability of strong microlensing effects depends on dark/stellar ratio

Custom microlensing maps are made for each system for a variety of dark/stellar ratios.

Strong demagnifications are unlikely for very high (100%) and very low (1%) stellar fractions.

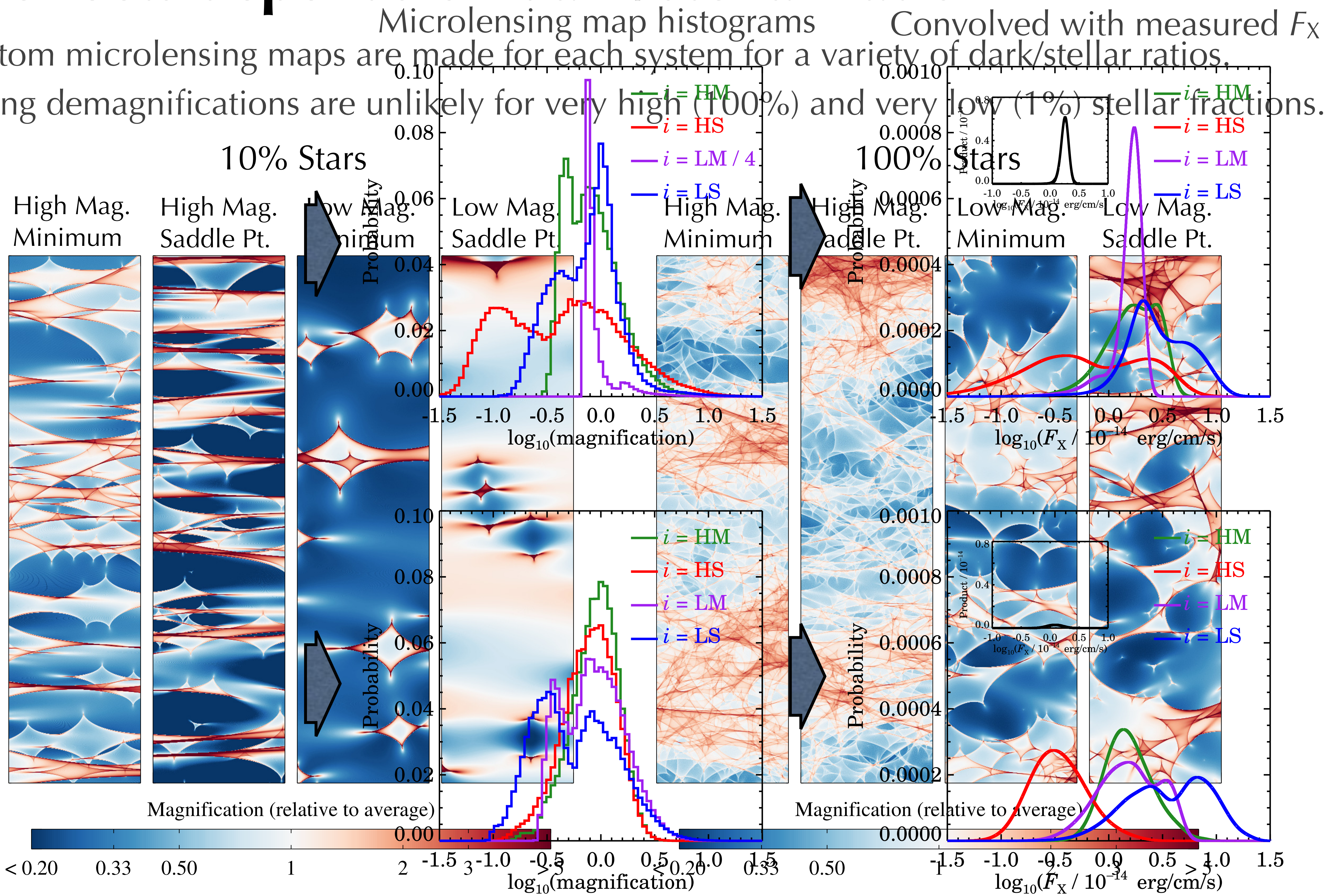

Stellar fraction decreases with $\langle R \rangle$ as expected

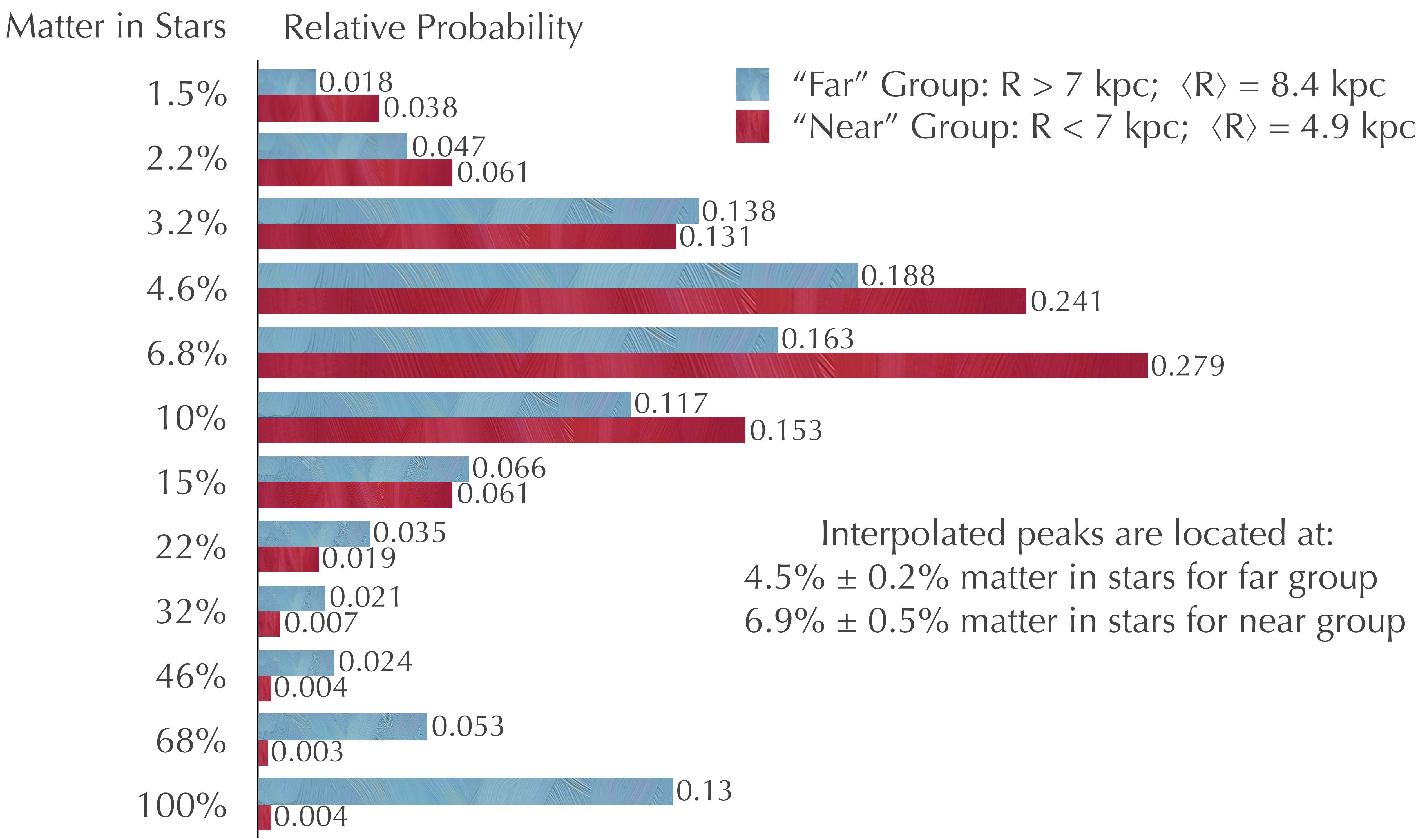

Interpolated peaks are located at:
4.5% ± 0.2% matter in stars for far group
6.9% ± 0.5% matter in stars for near group

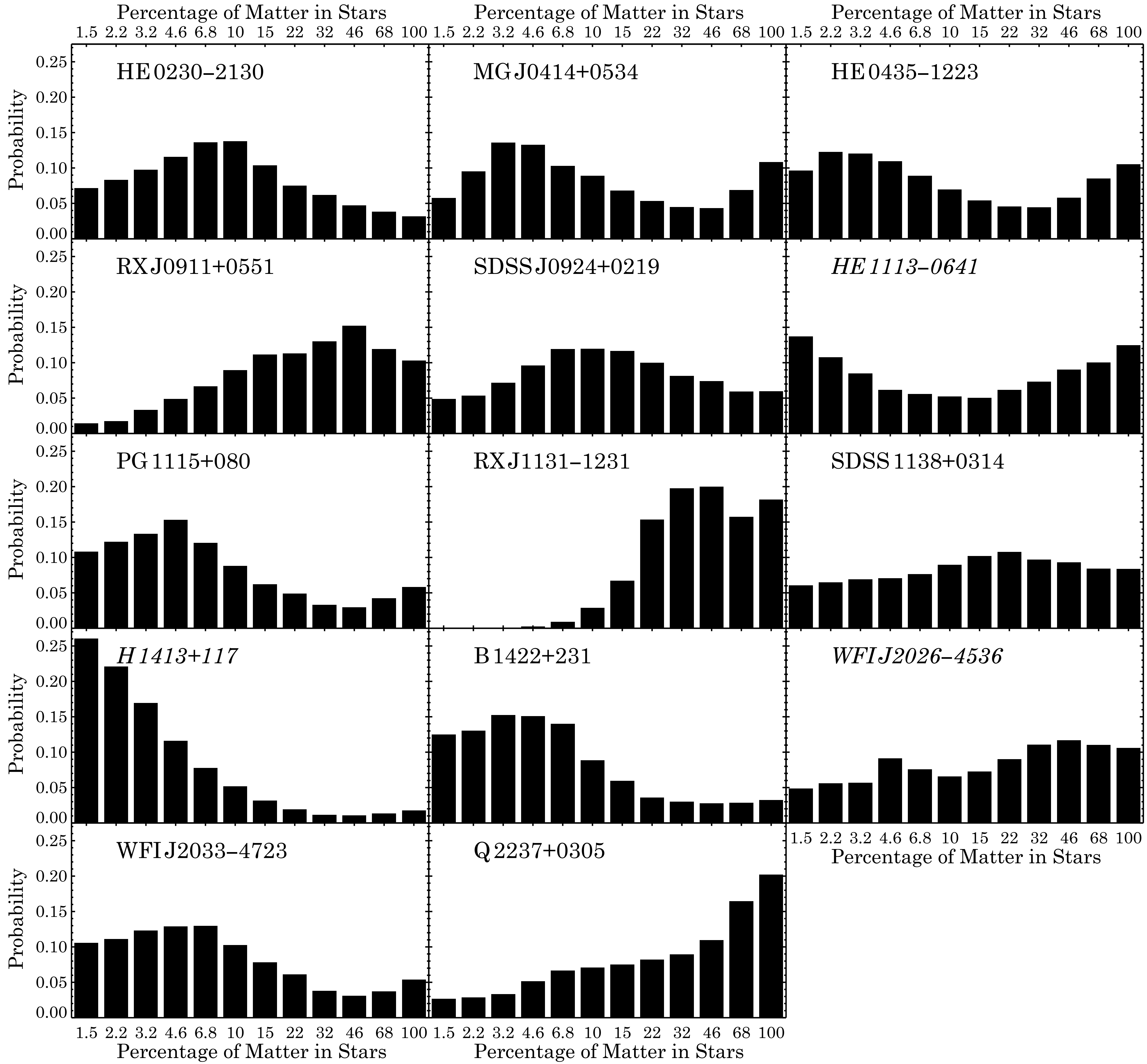

Percentage of Matter in Stars
Probability
HE 0230−2130
MG J0414+0534
HE 0435−1223
RX J0911+0551
SDSS J0924+0219
HE 1113−0641
PG 1115+080
RX J1131−1231
SDSS 1138+0314
H 1413+117
B 1422+231
WFI J2026−4536
WFI J2033−4723
Q 2237+0305
1.5 2.2 3.2 4.6 6.8 10 15 22 32 46 68 100
0.00 0.05 0.10 0.15 0.20 0.25

The larger the size of the source, the more the lensing effects are diminished

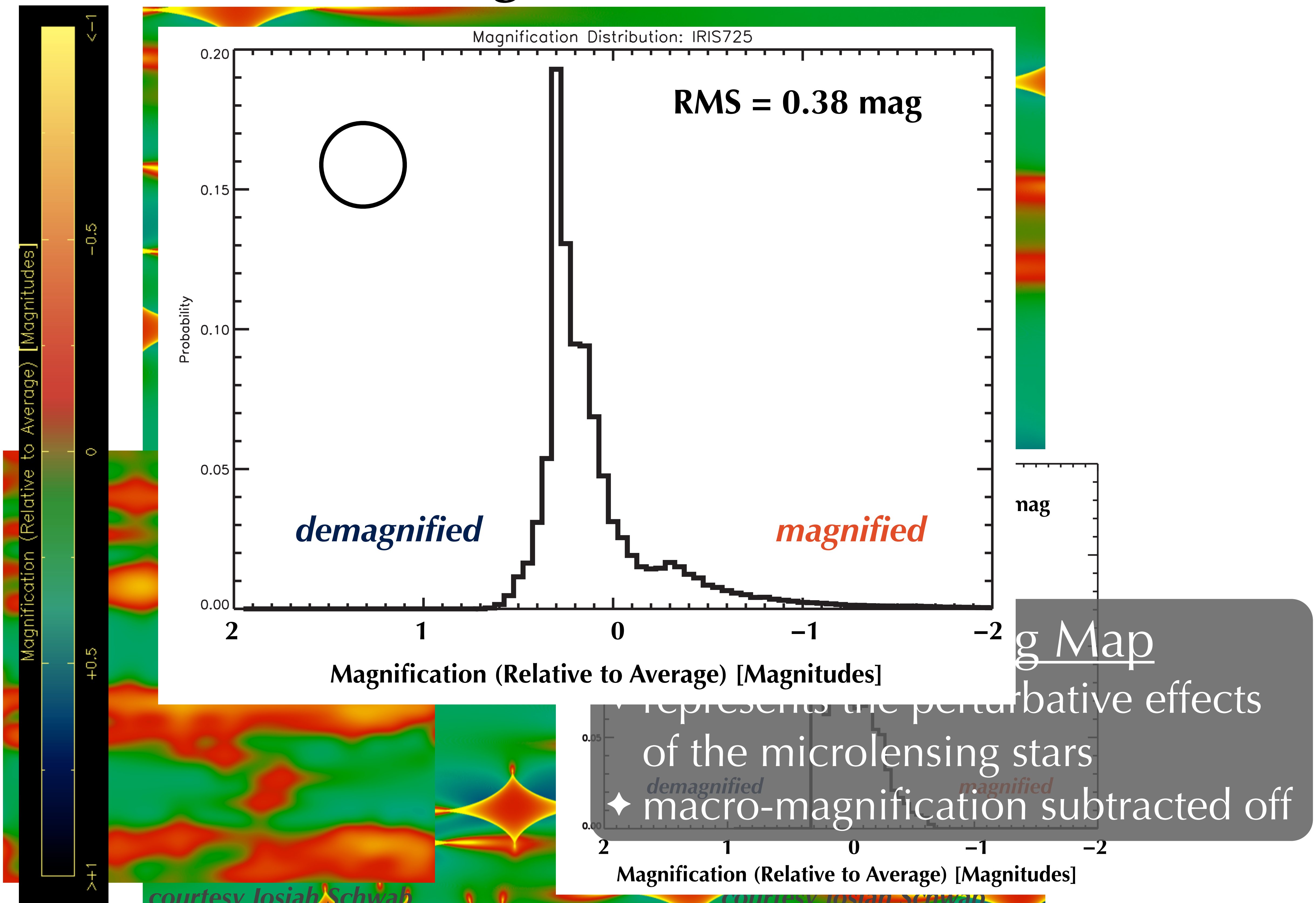

Possible caustic crossing is seen in PG 1115+080

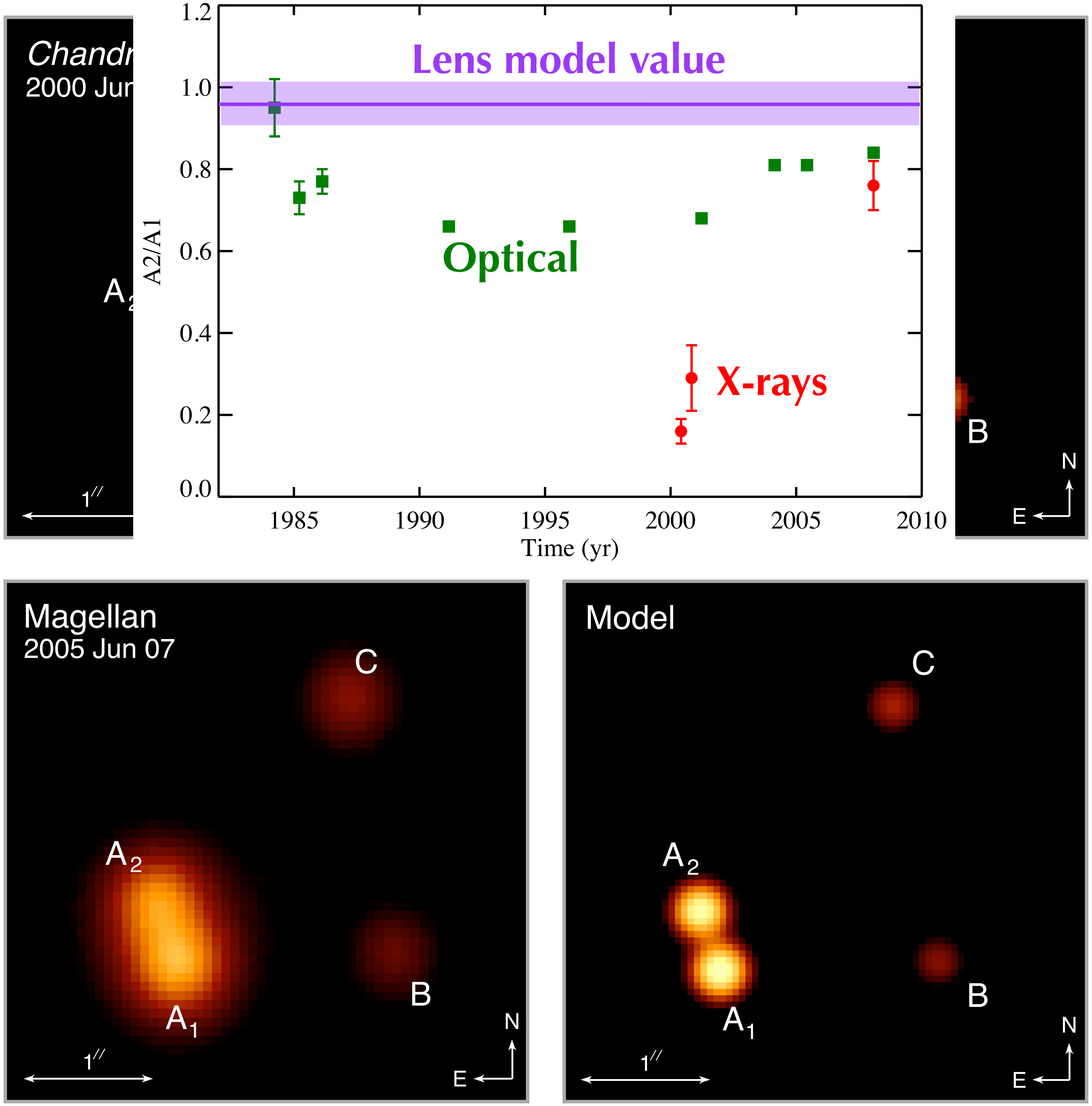

DP et al. 2008

Probability of microlensing depends on dark/stellar ratio

Custom microlensing maps are made for each system for a variety of dark/stellar ratios.
Strong demagnifications are unlikely for very high (100%) and very low (1%) stellar fractions.

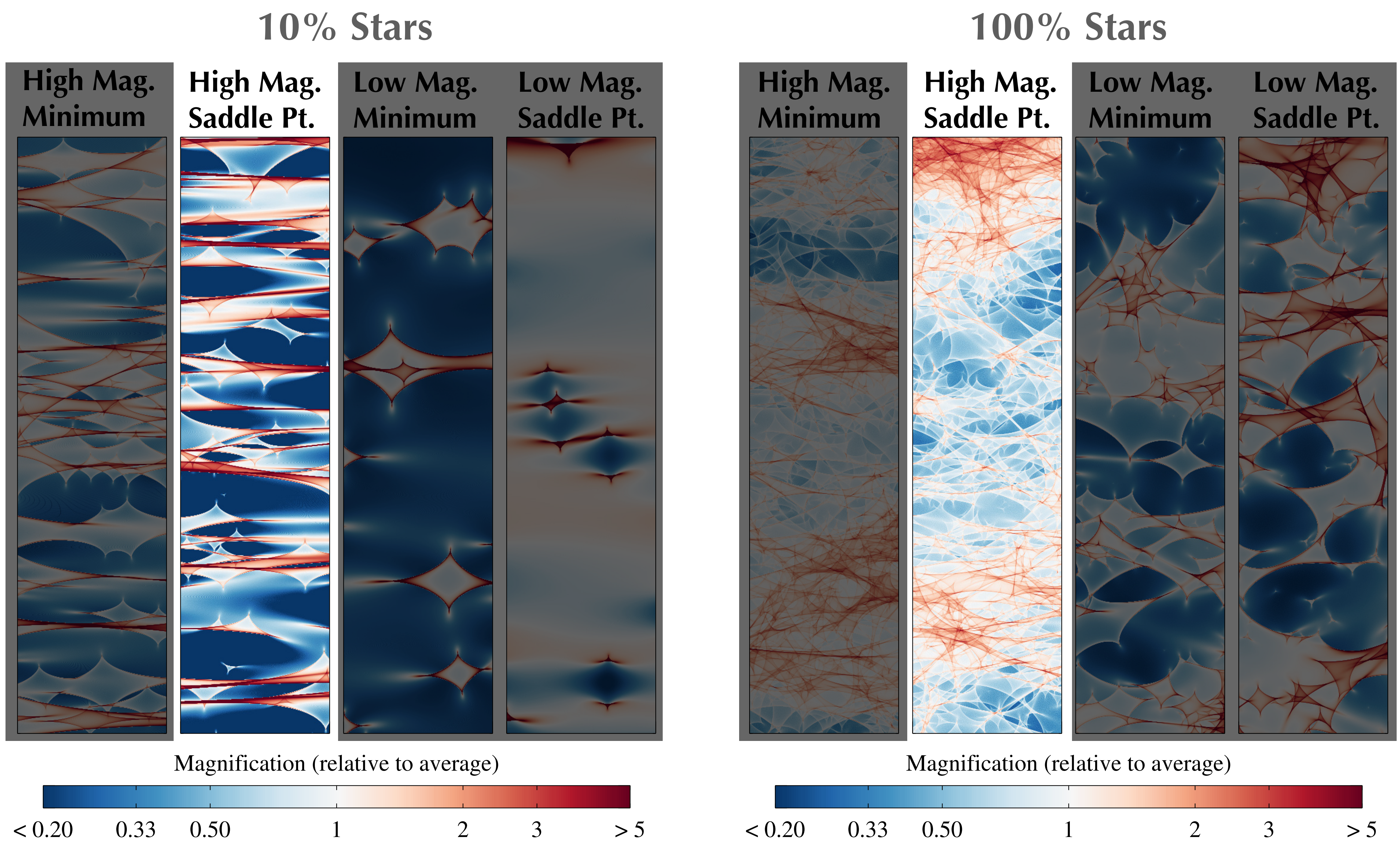

Multiply distributions to form joint P(F_X)

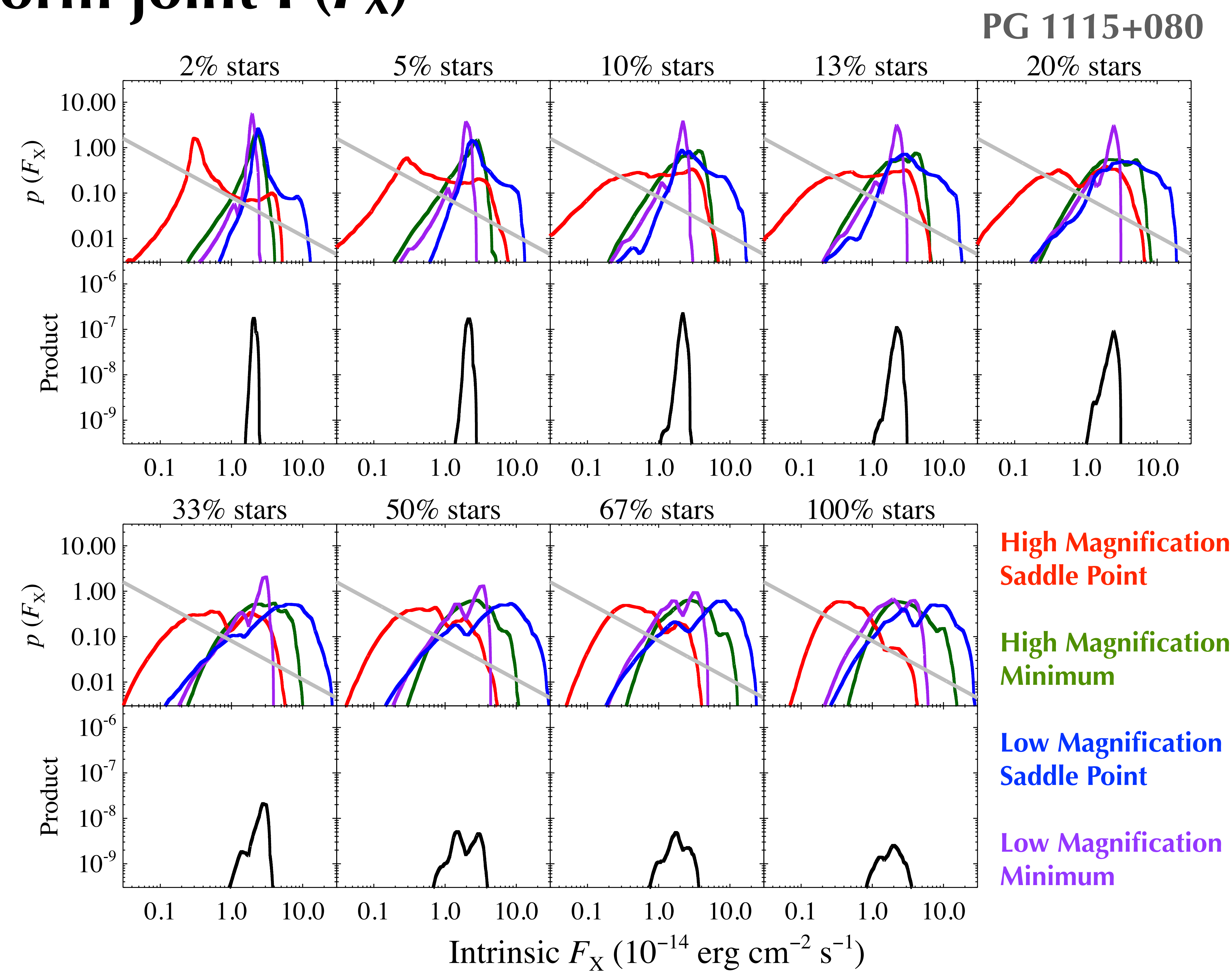

Marginalize over F_X to obtain likelihood of stellar fraction

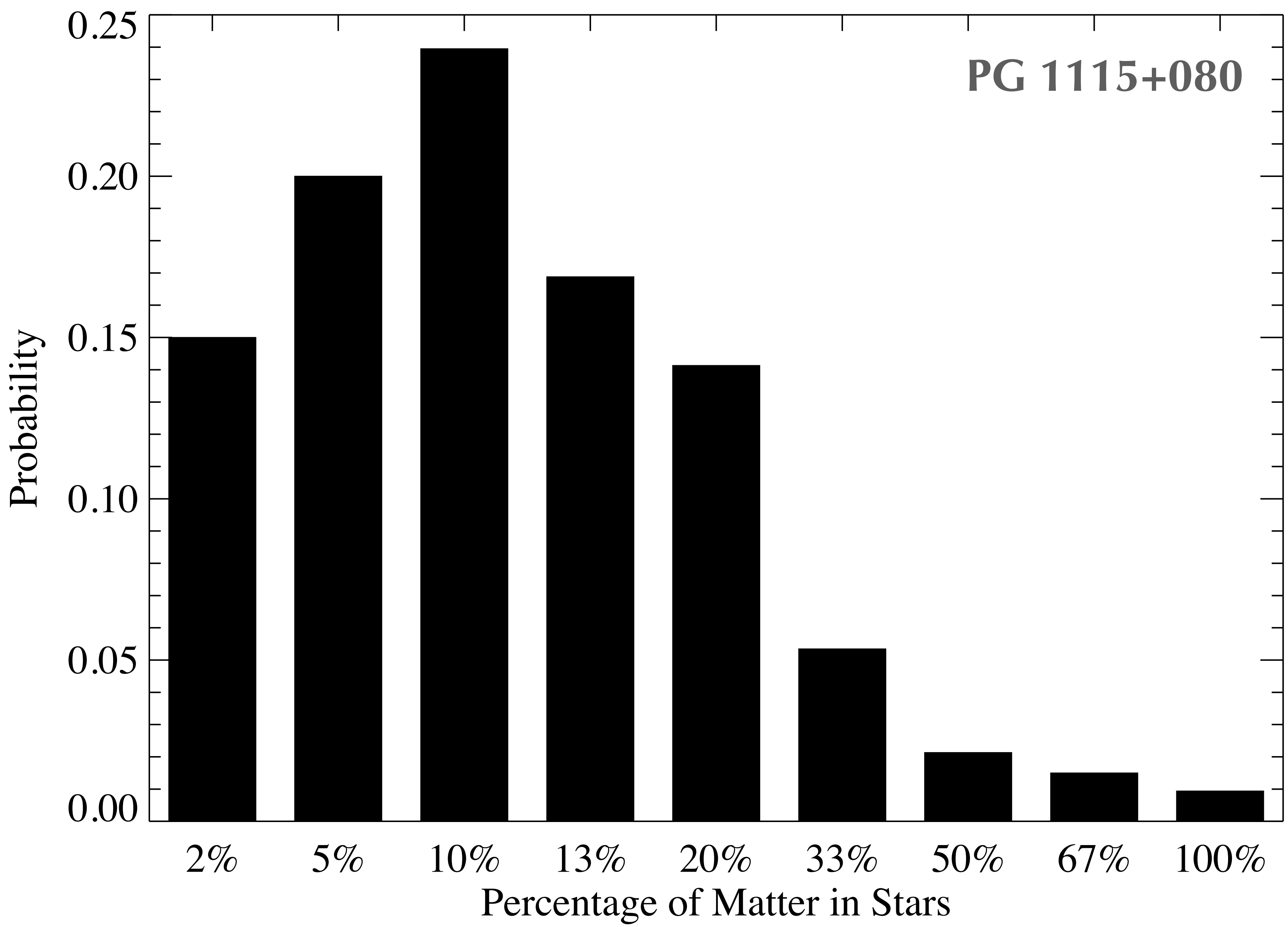

DP et al. 2009

Improved X-ray image modeling gives more precise measurement

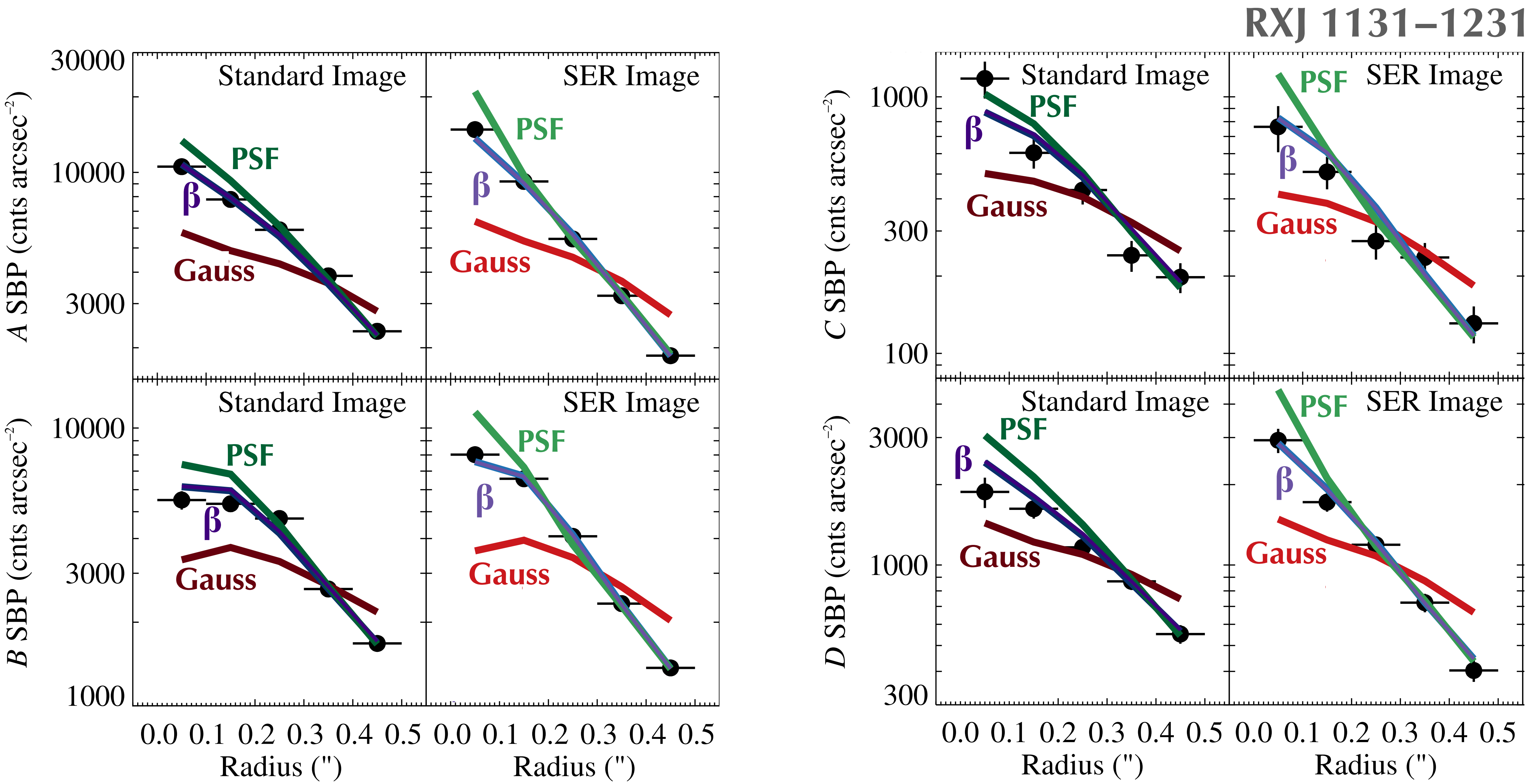

β profile: $I(r) = A(1 + (r/r_0)^2)^{-\beta}$

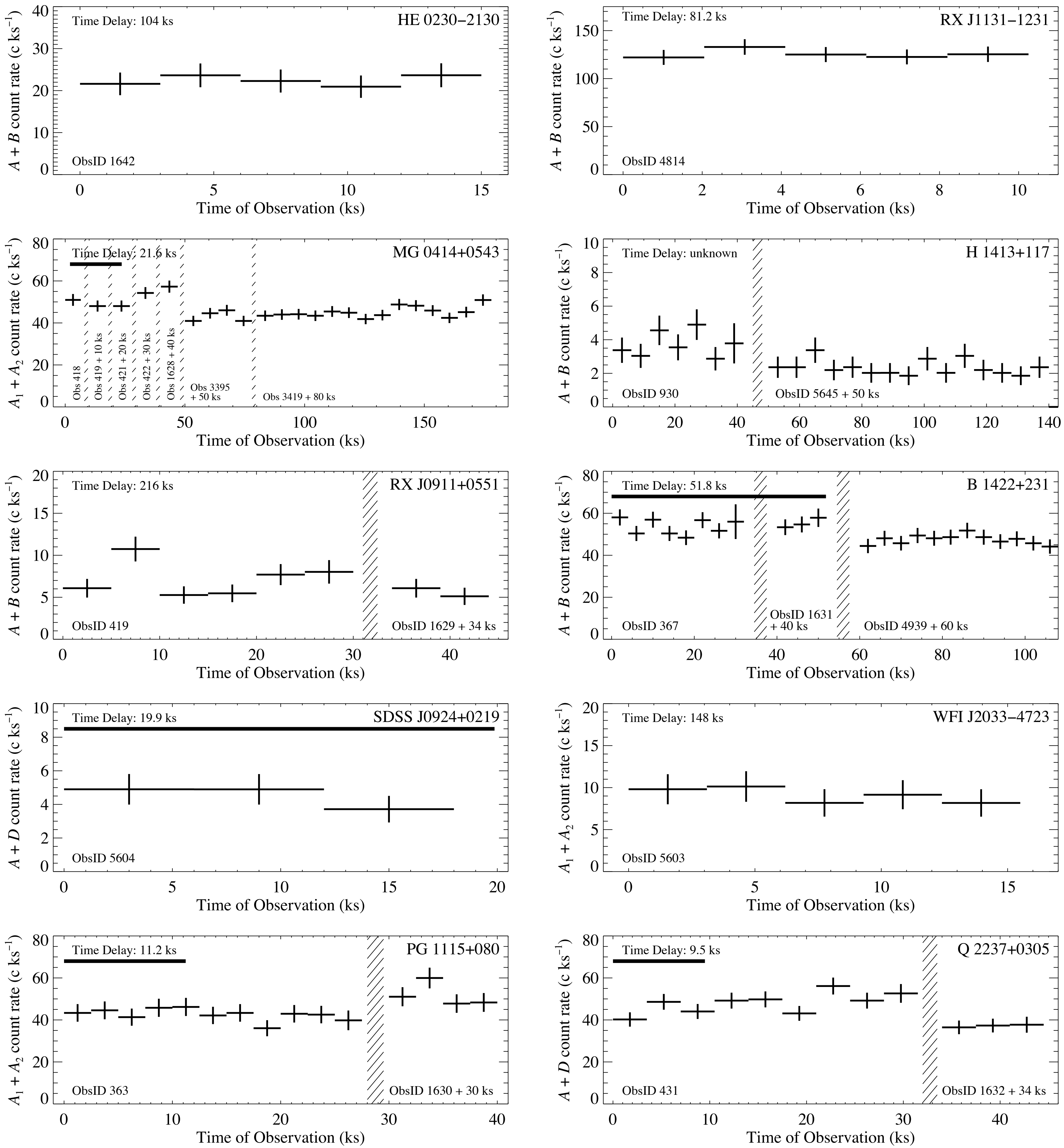

HE 0230−2130
Time Delay: 104 ks
ObsID 1642
RX J1131−1231
Time Delay: 81.2 ks
ObsID 4814
MG 0414+0543
Time Delay: 21.6 ks
Obs 418
Obs 419 + 10 ks
Obs 421 + 20 ks
Obs 422 + 30 ks
Obs 1628 + 40 ks
Obs 3395 + 50 ks
Obs 3419 + 80 ks
H 1413+117
Time Delay: unknown
ObsID 930
ObsID 5645 + 50 ks
RX J0911+0551
Time Delay: 216 ks
ObsID 419
ObsID 1629 + 34 ks
B 1422+231
Time Delay: 51.8 ks
ObsID 367
ObsID 1631 + 40 ks
ObsID 4939 + 60 ks
SDSS J0924+0219
Time Delay: 19.9 ks
ObsID 5604
WFI J2033−4723
Time Delay: 148 ks
ObsID 5603
PG 1115+080
Time Delay: 11.2 ks
ObsID 363
ObsID 1630 + 30 ks
Q 2237+0305
Time Delay: 9.5 ks
ObsID 431
ObsID 1632 + 34 ks
A + B count rate (c ks−1)
A1 + A2 count rate (c ks−1)
A + D count rate (c ks−1)
Time of Observation (ks)

DP et al. 2007

Galaxy Mass Profiles from (SLACS)

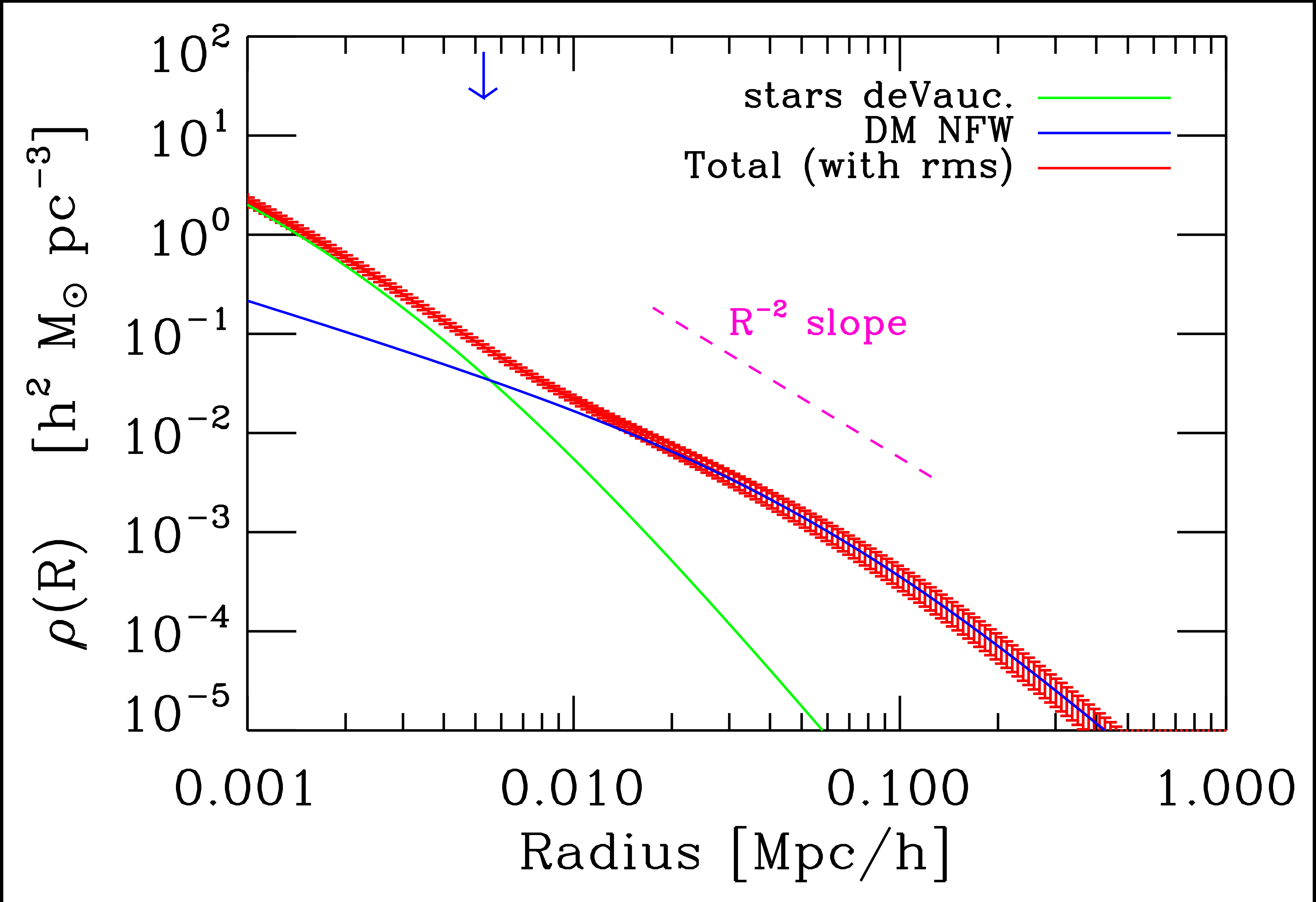

Gavazzi et al. 2007

The Sizes of Quasar Emission Regions

We calculate $R_{1/2}$ according to:

$$\frac{\int_{r_0}^{r_{1/2}} \left[e^{h\nu(1+z)/kT(r)} - 1\right]^{-1} r dr}{\int_{r_0}^{\infty} \left[e^{h\nu(1+z)/kT(r)} - 1\right]^{-1} r dr} = \frac{1}{2}$$

using a Shakura-Sunyaev model:

$$T(r) = \left[\frac{3GM_{\mathrm{BH}}\dot{M}}{8\pi\sigma r^3}\right]^{1/4} \left(1 - \sqrt{r_0/r}\right)^{1/4}$$

Estimate L_{Bol} using $9[\lambda F_\lambda]_{5100} 4\pi D_{\mathrm{L}}^2$ *Kaspi et al. 2000*

Take $L_{\mathrm{Bol}}/L_{\mathrm{Edd}} \equiv f_{\mathrm{E}} = 0.25$ *Kollmeier et al. 2006*

Take radiative efficiency $\eta = 0.15$ *Yu & Tremaine 2002*

$\rightarrow a = 0.88$ and $r_0 \approx 2.5\ R_{\mathrm{g}}$

Assumptions: How does choice of η and f_E affect $R_{1/2}$?

- Can use $T(r)$ to find radius where $T/(1+z) = h\nu/k_B$
- To good approximation, this radius $\propto R_{1/2}$
- Neglecting the factor of $(1-\sqrt{r_0/r})^{1/4}$ in $T(r)$, we find

$$R_{1/2} \propto (M_{BH}\,\dot{M})^{1/3}$$

- Since $M_{BH} \propto L_{bol}/f_E$ and $\dot{M} \propto L_{bol}/\eta$

$$\Rightarrow \; R_{1/2} \propto (f_E\,\eta)^{-1/3}$$